Supporting Information for

Polyoxometalate-Based Ionic Liquids: Efficient Reversible Phase Transformation-type Catalysts for Thiolation of Alcohols to Construct C-S Bond

Jikun Li,† Junwei Ma,† Chuanping Wei, Zebao Zheng, Yinfeng Han,* Huiping Wang, Xueshen Wang, and Changwen Hu*

†J. Li and J. Ma contributed equally. E-mail address: hanyf1978@163.com, cwhu@bit.edu.cn

Table of contents

S1. Spectroscopic data of $[MIMPS]_3PW_{12}O_{40}$, $[EIMPS]_3PW_{12}O_{40}$ and $[PIMPS]_3PW_{12}O_{40}$.

$[MIMPS]_3PW_{12}O_{40}$: Yied: 94%. FT-IR (KBr, cm^{-1}): 3445 (br, O-H), 1627, 1568, 1462, 1210, 1167, 1082, 981, 895, 808, 615, 522. ^1H NMR (500 MHz, DMSO-d_6) δ 9.13-9.08 (m, 1H), 7.81-7.74 (m, 1H), 7.71-7.67 (m, 1H), 4.30 (t, *J*=7.0 Hz, 2H), 3.85 (s, 3H), 2.45 (t, *J*=7.2 Hz, 2H), 2.09 (p, *J*=7.0 Hz, 2H). ^{13}C NMR (126 MHz, DMSO-d_6) δ 137.19, 124.06, 122.78, 48.19, 47.76, 36.20, 26.58. Positive-ion electrospray ionization mass spectrometry (ESI-MS) m/z: 205.05 ($MIMPS^+$). Negative-ion electrospray ionization mass spectrometry (ESI-MS) m/z: 959.72 ($PW_{12}O_{40}^{3-}$).[1]

$[EIMPS]_3PW_{12}O_{40}$: Yied: 93%. FT-IR (KBr, cm^{-1}): 3436 (br, O-H), 1628, 1558, 1454, 1202, 1160, 1083, 972, 902, 804, 594, 518. ^1H NMR (500 MHz, DMSO-d_6) δ 9.19 (s, 1H), 7.80 (s, 2H), 4.30 (t, *J*=7.0 Hz, 2H), 4.20 (q, *J*=7.3 Hz, 2H), 2.45 (t, *J*=7.3 Hz, 2H), 2.11 (p, *J*=7.2 Hz, 2H), 1.43 (t, *J*=7.2 Hz, 3H). ^{13}C NMR (126 MHz, DMSO-d_6) δ 136.32, 122.92, 122.55, 48.29, 47.83, 44.70, 26.52, 15.46. Positive-ion electrospray ionization mass spectrometry (ESI-MS) m/z: 219.08 ($EIMPS^+$). Negative-ion electrospray ionization mass spectrometry (ESI-MS) m/z: 959.72 ($PW_{12}O_{40}^{3-}$).

$[PIMPS]_3PW_{12}O_{40}$: Yied: 95%. FT-IR (KBr, cm^{-1}): 34436 (br, O-H), 1627, 1559, 1455, 1209, 1165, 1084, 985, 904, 811, 595, 510. ^1H NMR (500 MHz, DMSO-d_6) δ 9.20 (d, *J*=1.7 Hz, 1H), 7.84-7.77 (m, 2H), 4.30 (t, *J*=7.0 Hz, 2H), 4.13 (t, *J*=7.1 Hz, 2H), 2.43 (t, *J*=7.2 Hz, 2H), 2.10 (tt, *J*=7.0 Hz, *J*=7.2 Hz,2H), 1.82 (h, *J*=7.3 Hz, 2H), 0.85 (t, *J*=7.4 Hz, 3H). ^{13}C NMR (126 MHz, DMSO-d_6) δ 136.67, 123.01, 122.88, 50.80, 48.32, 47.81, 26.59, 23.23, 10.90. Positive-ion electrospray ionization mass spectrometry (ESI-MS) m/z: 233.10 ($PIMPS^+$). Negative-ion electrospray ionization mass spectrometry (ESI-MS) m/z: 959.72 ($PW_{12}O_{40}^{3-}$).

Table S1. Optimization of types of catalysts for the reaction of 2-phenyl-2-propanol and 4-fluorobenzenethiol.[a]

Entry	Catalyst	Yield (%)[b]
1	$[MIMPS]_3PW_{12}O_{40}$	91.8
2	$[EIMPS]_3PW_{12}O_{40}$	92.5
3	$[PIMPS]_3PW_{12}O_{40}$	97.5

Reaction conditions: 2-phenyl-2-propanol (0.6 mmol), thiols (0.5 mmol), catalyst (5 mol%, molar ratio based on thiol and $PW_{12}O_{40}^{3-}$), 70 °C, 2 mL acetonitrile, 1 h. [b]GC yield, biphenyl as internal standard.

Table S2. Optimization of the loading of $[PIMPS]_3PW_{12}O_{40}$ for the reaction of 2-phenyl-2-propanol and 4-fluorobenzenethiol.[a]

Entry	Catalyst loading (%)	Yield (%)[b]
1	Blank	NR
2	3	95.8
3	5	97.5
4	7	98.7

Reaction conditions: 2-phenyl-2-propanol (0.6 mmol), thiols (0.5 mmol), $[PIMPS]_3PW_{12}O_{40}$ (molar ratio based on thiol and $PW_{12}O_{40}^{3-}$), 70 °C, 2 mL acetonitrile, 1 h. [b]GC yield, biphenyl as internal standard.

Table S3. Optimization of temperature for the reaction of 2-phenyl-2-propanol and 4-fluorobenzenethiol.[a]

Entry	Temperature (°C)	Yield (%)[b]
1	25 (r.t.)	61.2
2	50	80.6
3	70	97.5
4	90	98.2

Reaction conditions: 2-phenyl-2-propanol (0.6 mmol), thiols (0.5 mmol), $[PIMPS]_3PW_{12}O_{40}$ (5 mol%, molar ratio based on thiol and $PW_{12}O_{40}^{3-}$), 2 mL acetonitrile, 1 h. [b]GC yield, biphenyl as internal standard.

Table S4. Optimization of the solvent used for the reaction of 2-phenyl-2-propanol and 4-fluorobenzenethiol.[a]

Entry	Solvent	Yield (%)[b]
1	CH_2Cl_2	40.6
2	CH_3OH	< 5
3	CH_3CN	97.5

Reaction conditions: 2-phenyl-2-propanol (0.6 mmol), thiols (0.5 mmol), $[PIMPS]_3PW_{12}O_{40}$ (5 mol%, molar ratio based on thiol and $PW_{12}O_{40}^{3-}$), 70 °C, 1 h. [b]GC yield, biphenyl as internal standard.

Table S5. Optimization of the time for the reaction of 2-phenyl-2-propanol and 4-fluorobenzenethiol.[a]

Entry	Time (h)	Yield (%)[b]
1	0.5	94.4
2	1	97.5
3	1.5	98.4

Reaction conditions: 2-phenyl-2-propanol (0.6 mmol), thiols (0.5 mmol), $[PIMPS]_3PW_{12}O_{40}$ (5 mol%, molar ratio based on thiol and $PW_{12}O_{40}^{3-}$), 70 °C, 2 mL acetonitrile. [b]GC yield, biphenyl as internal standard.

Table S6. Optimization of the molar ratio of 2-phenyl-2-propanol and 4-fluorobenzenethiol.[a]

Entry	Molar ratio (alcohol/thiol)	Yield (%)[b]
1	1:1 (alcohol 0.5 mmol)	93.5
2	1.2:1 (alcohol 0.6 mmol)	97.5

Reaction conditions: $[PIMPS]_3PW_{12}O_{40}$ (5 mol%, molar ratio based on thiol and $PW_{12}O_{40}^{3-}$), 70 °C, 2 mL acetonitrile, 1 h. [b]GC yield, biphenyl as internal standard.

Figure S1. Quantitative standard curve used for GC.

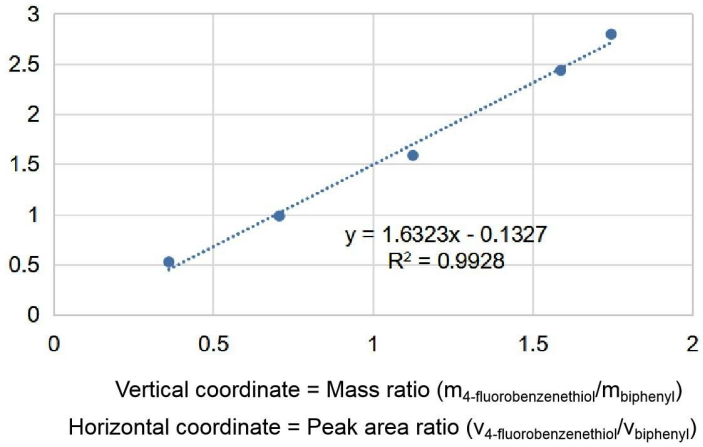

Figure S2. FT-IR spectra of $[MIMPS]_3PW_{12}O_{40}$.

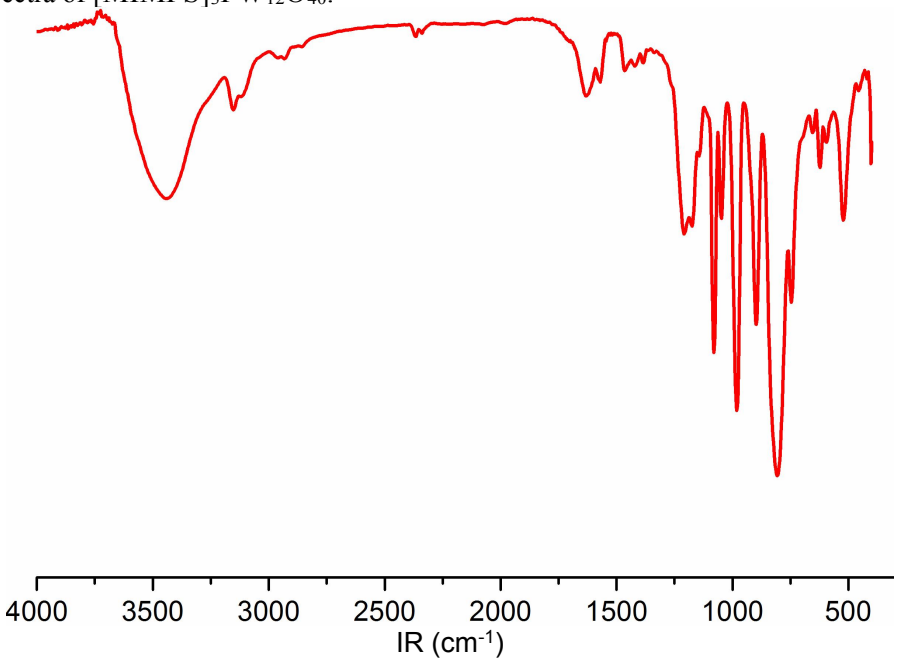

Figure S3. FT-IR spectra (cm^{-1}) of $[EIMPS]_3PW_{12}O_{40}$.

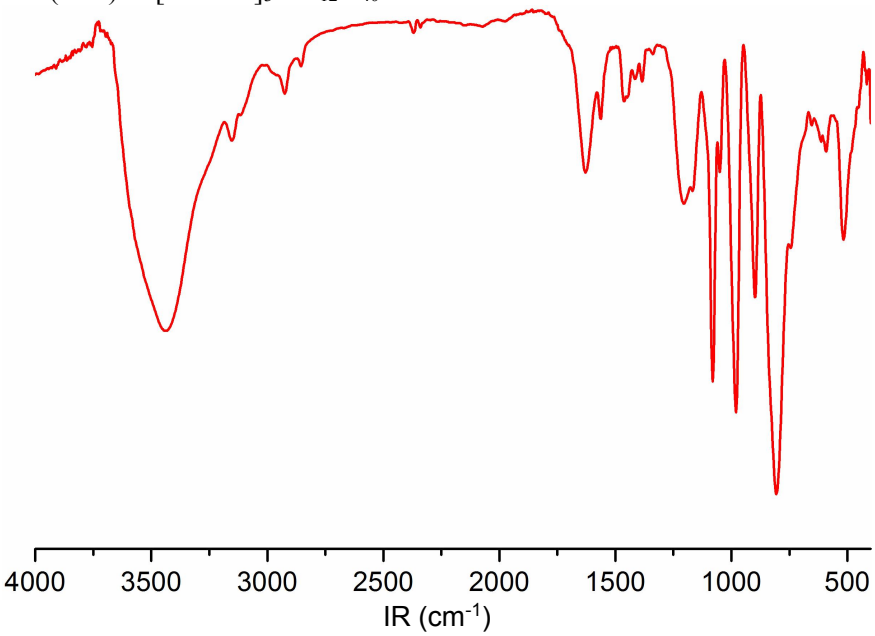

Figure S4. FT-IR spectra (cm^{-1}) of $[PIMPS]_3PW_{12}O_{40}$.

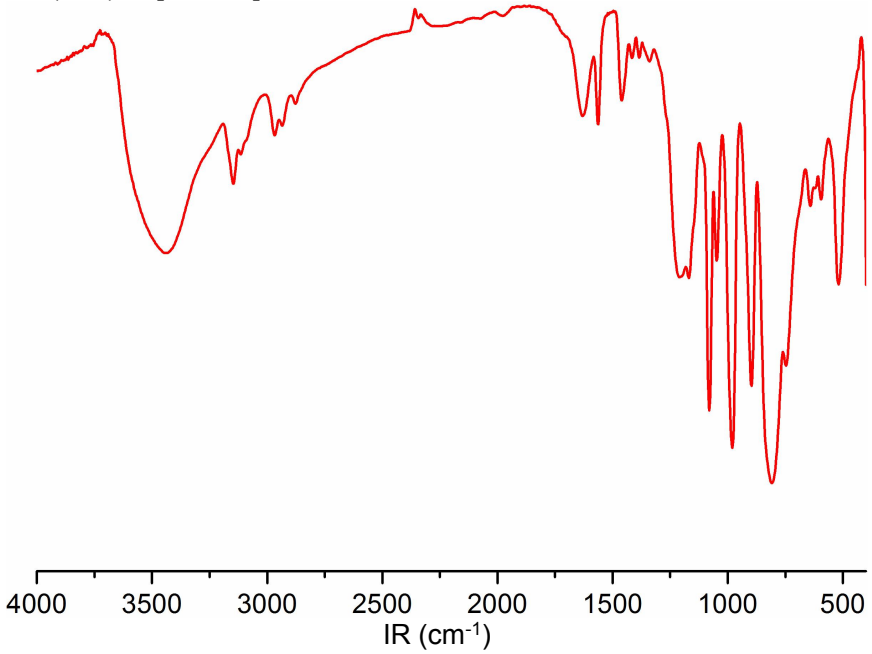

Figure S5. NMR spectra of $[MIMPS]_3PW_{12}O_{40}$.

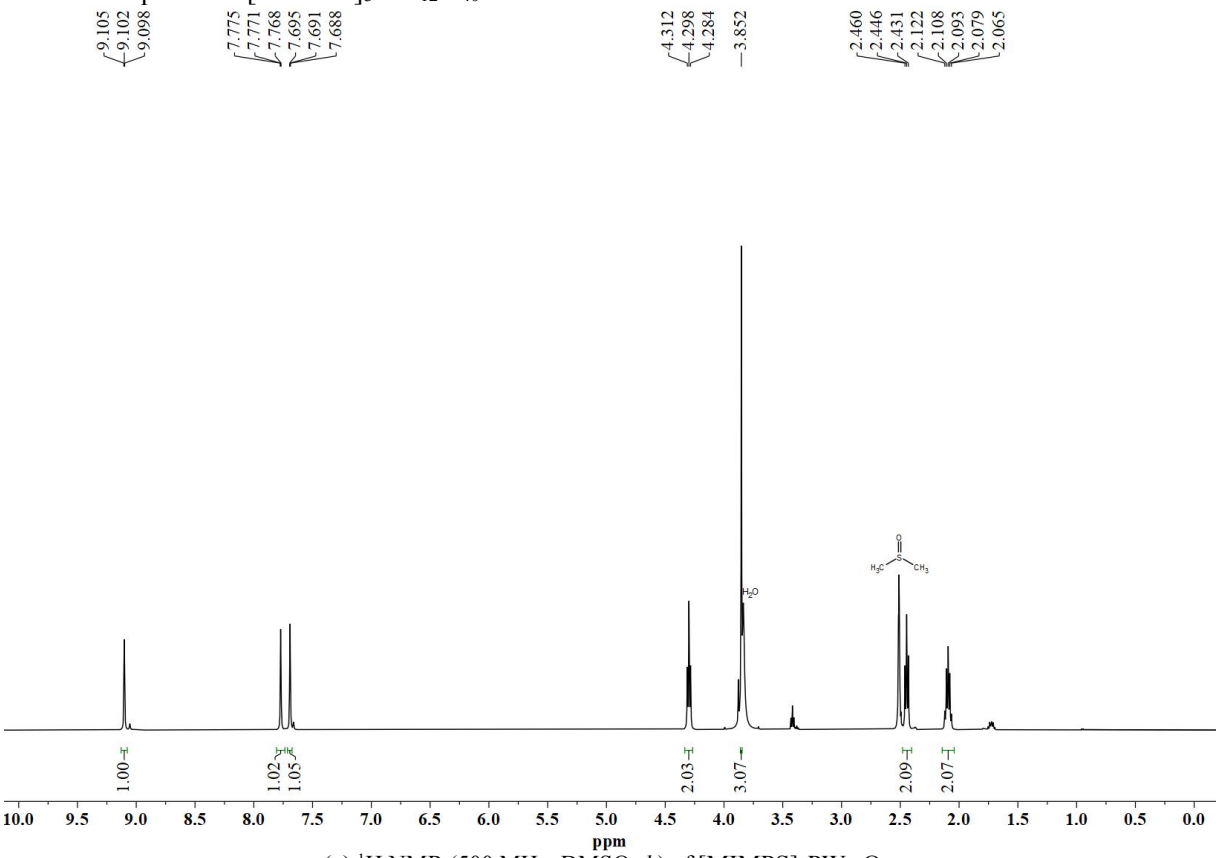

(a) ^{1}H NMR (500 MHz, DMSO-d_6) of $[MIMPS]_3PW_{12}O_{40}$.

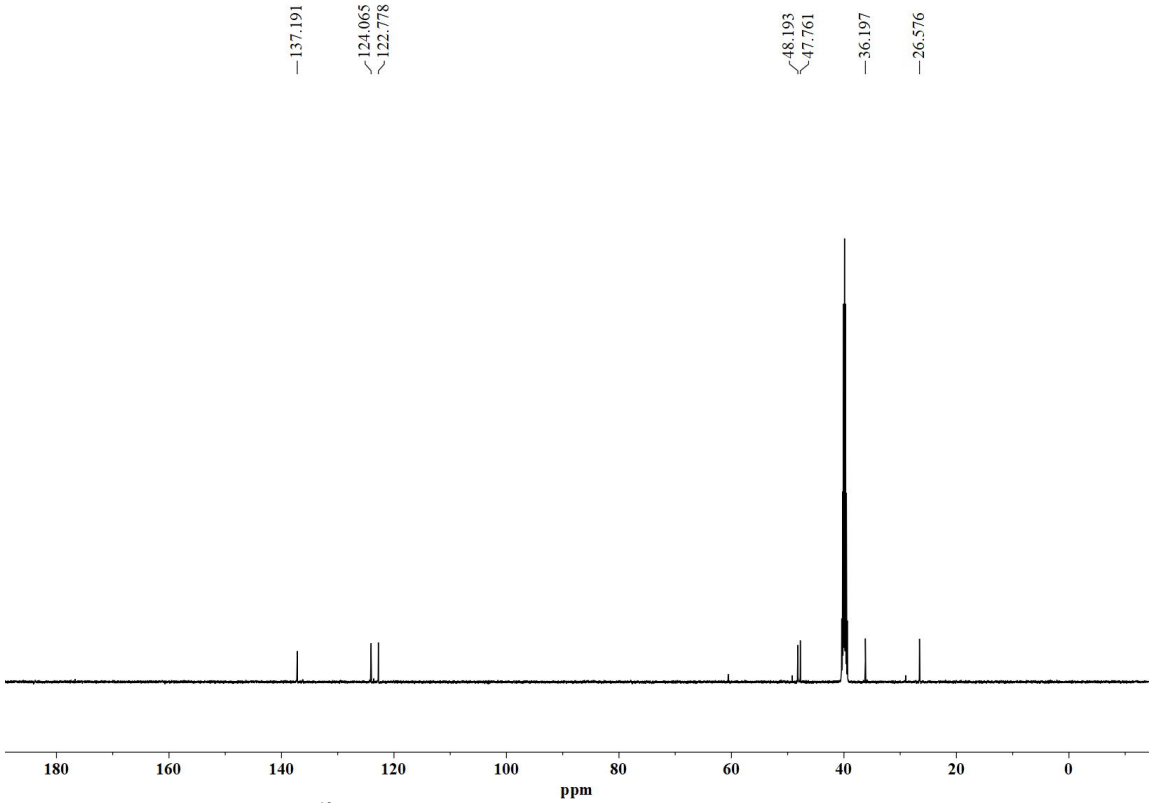

(b) ^{13}C NMR (126 MHz, DMSO-d_6) of $[MIMPS]_3PW_{12}O_{40}$.

Figure S6. NMR spectra of $[EIMPS]_3PW_{12}O_{40}$.

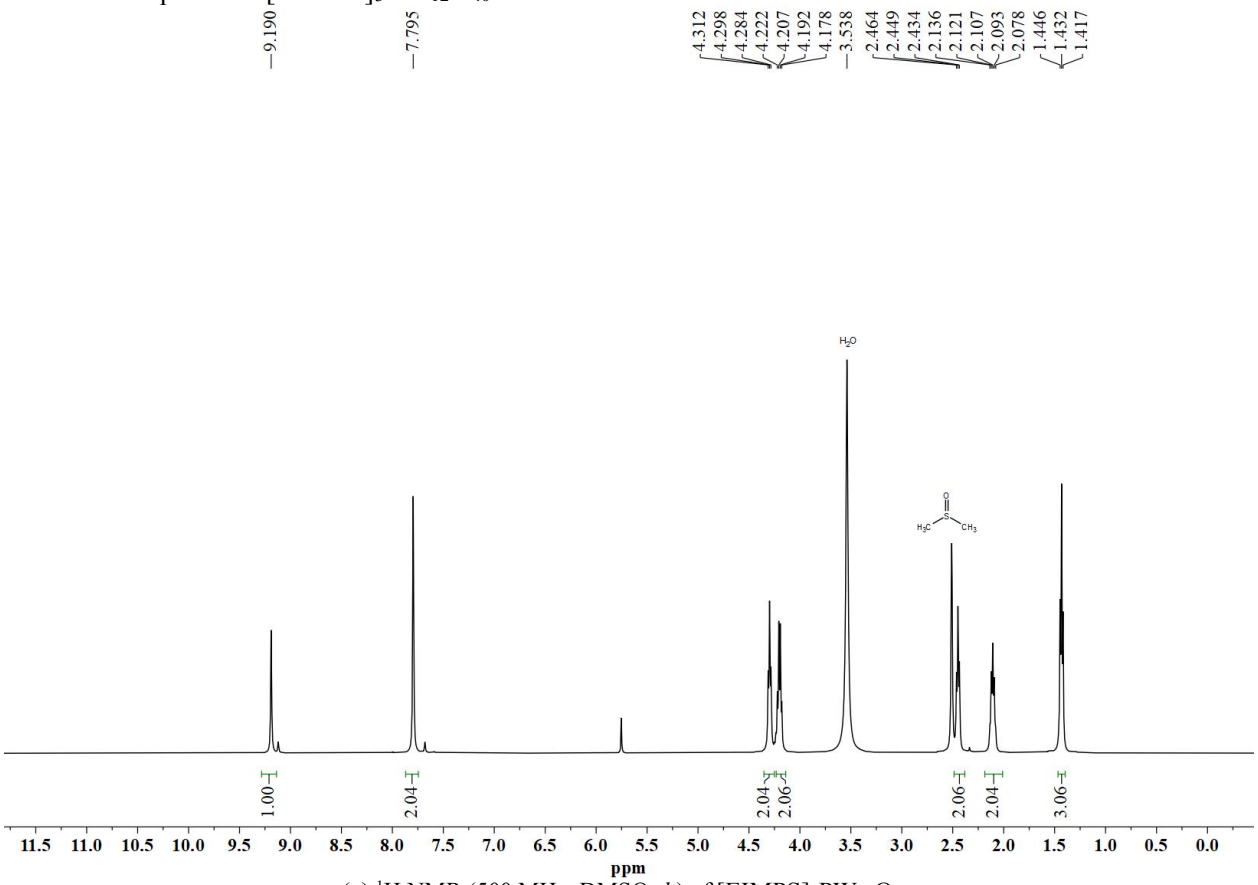

(a) ^{1}H NMR (500 MHz, DMSO-d_6) of $[EIMPS]_3PW_{12}O_{40}$.

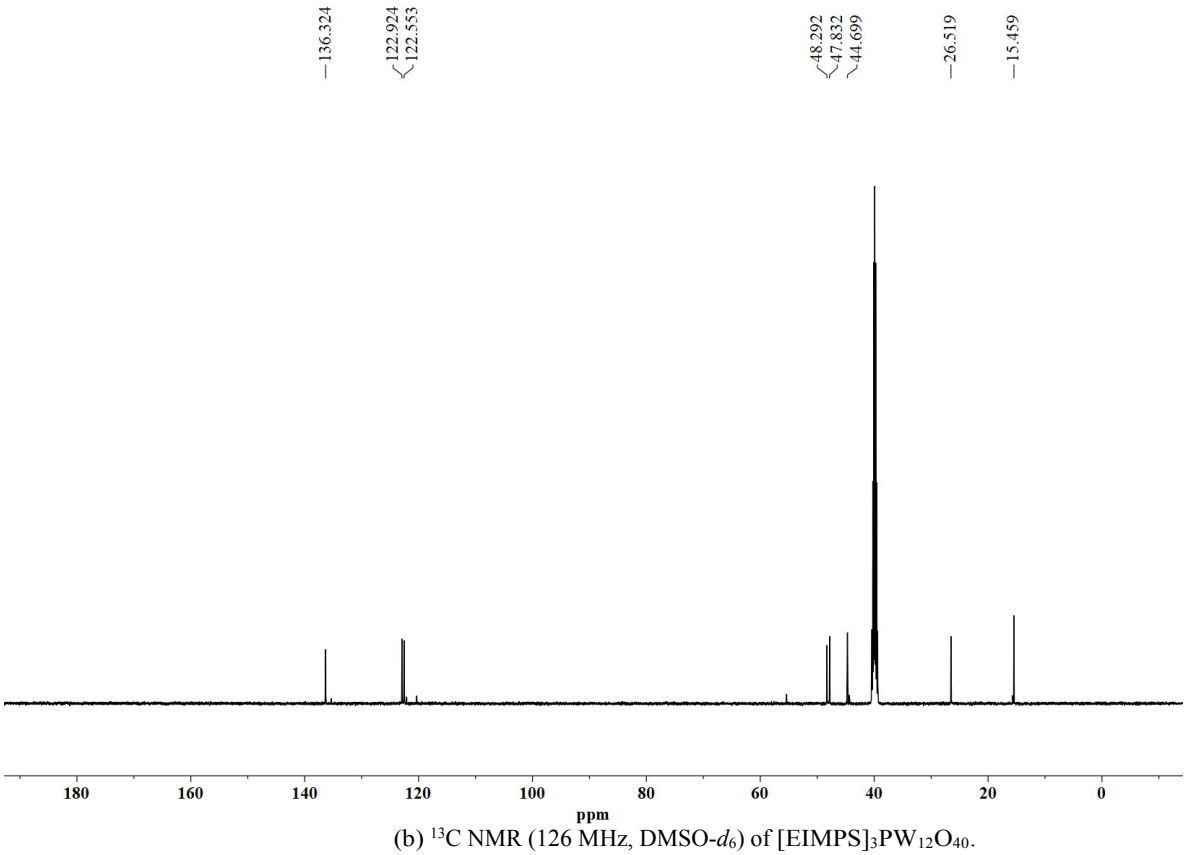

(b) ^{13}C NMR (126 MHz, DMSO-d_6) of $[EIMPS]_3PW_{12}O_{40}$.

Figure S7. NMR spectra of $[PIMPS]_3PW_{12}O_{40}$.

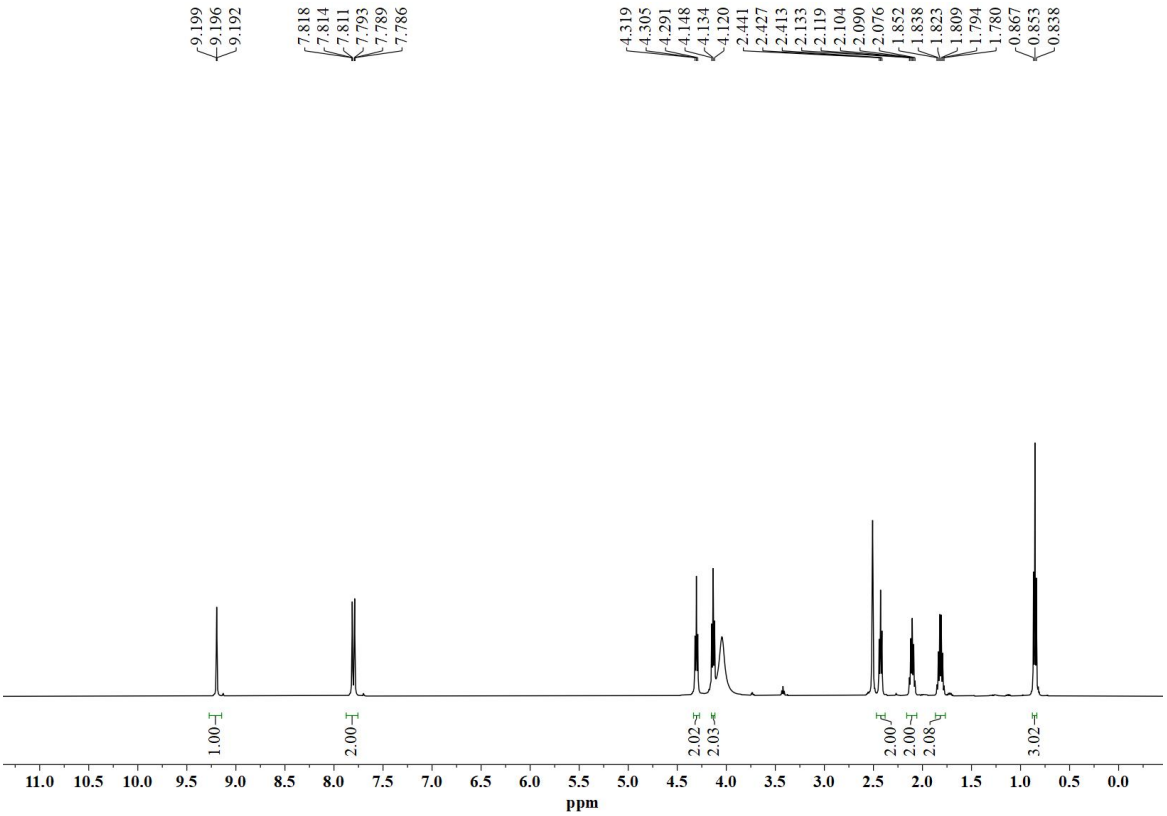

(a) ^{1}H NMR (500 MHz, DMSO-d_6) of $[PIMPS]_3PW_{12}O_{40}$.

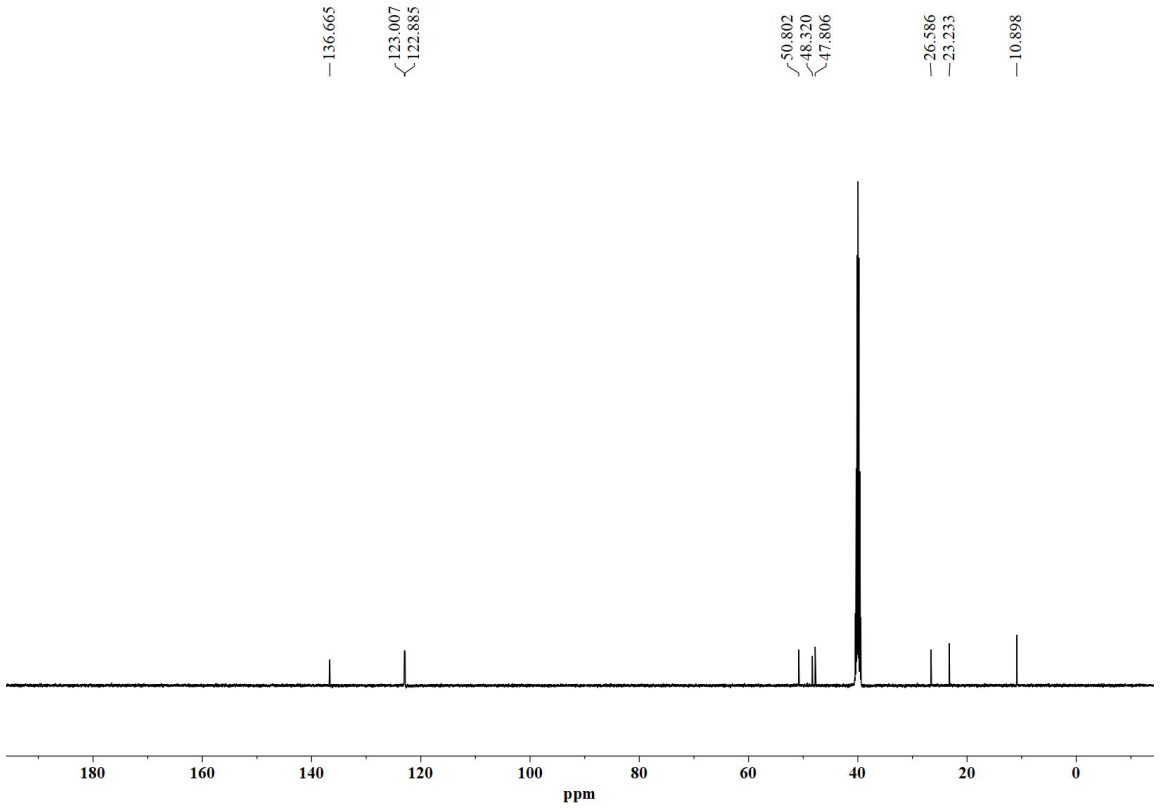

(b) ^{13}C NMR (126 MHz, DMSO-d_6) of $[PIMPS]_3PW_{12}O_{40}$.

Figure S8. ESI-MS of $[MIMPS]_3PW_{12}O_{40}$.

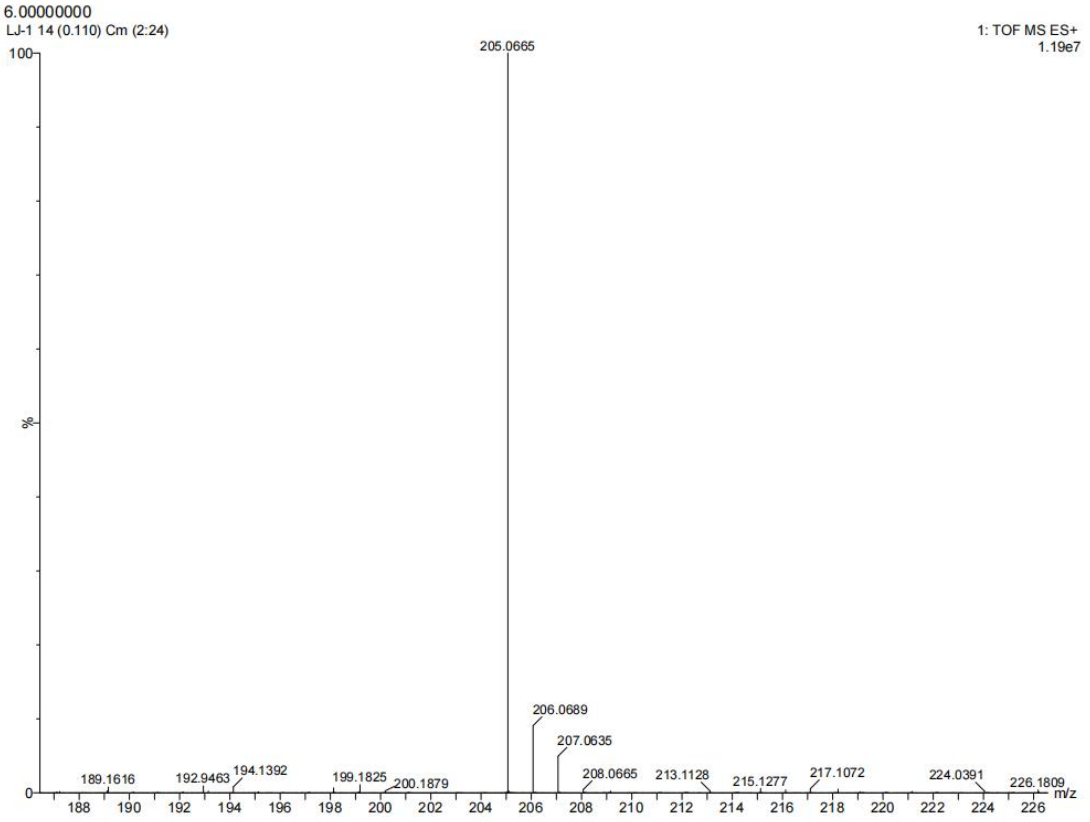

(a) Positive-ion ESI-MS of $[MIMPS]_3PW_{12}O_{40}$.

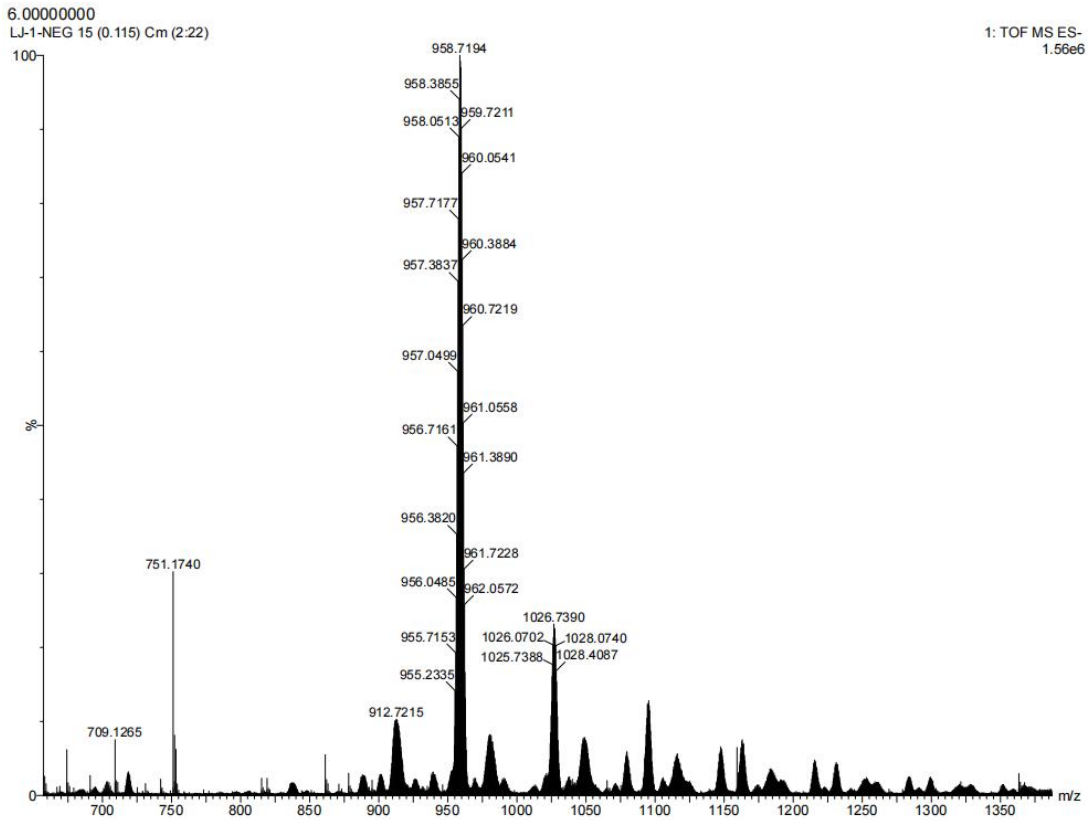

(b) Negative-ion ESI-MS of $[MIMPS]_3PW_{12}O_{40}$.

Figure S9. ESI-MS of $[EIMPS]_3PW_{12}O_{40}$.

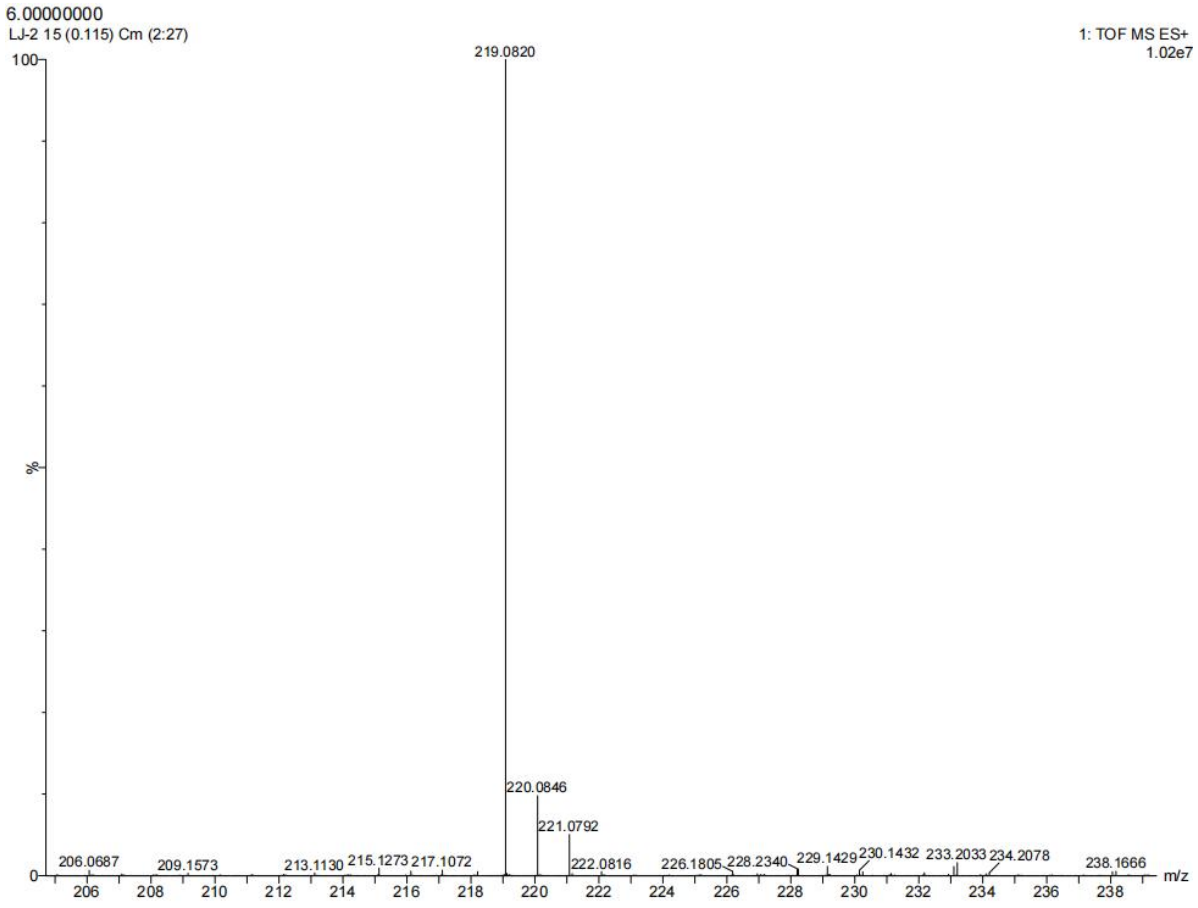

(a) Positive-ion ESI-MS of $[EIMPS]_3PW_{12}O_{40}$.

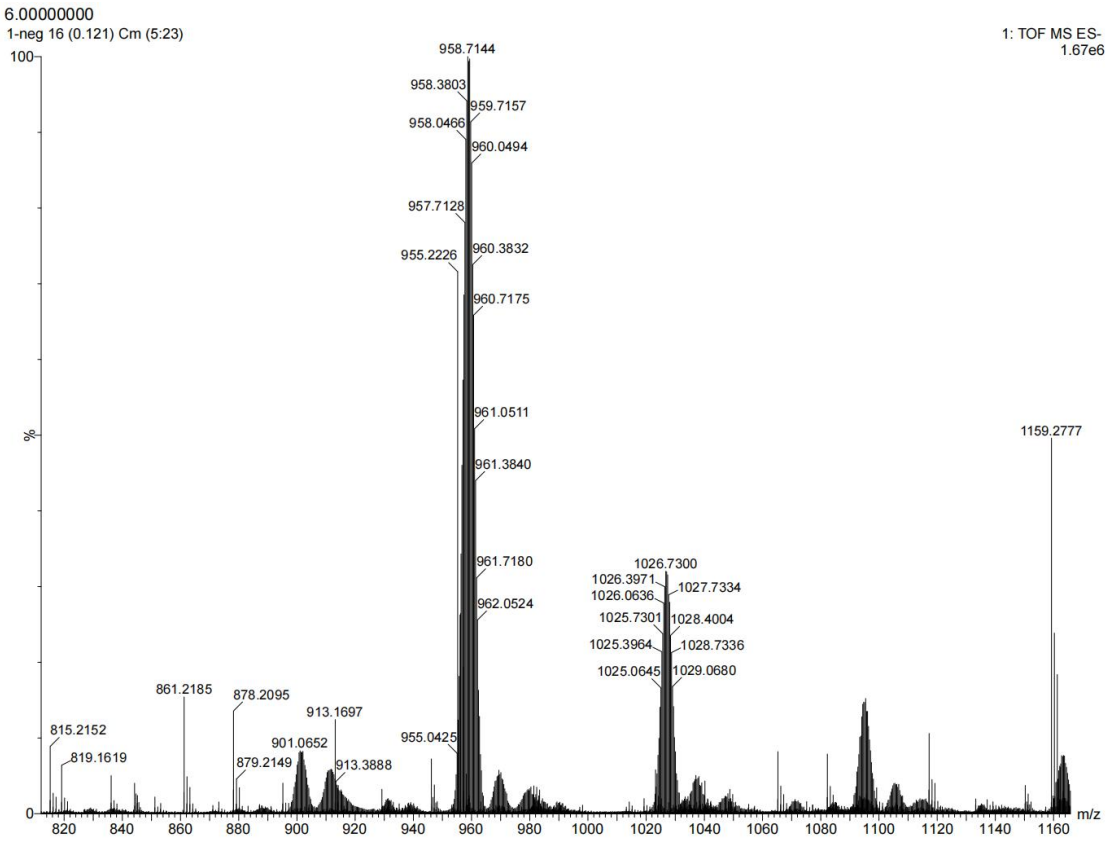

(b) Negative-ion ESI-MS of $[EIMPS]_3PW_{12}O_{40}$.

Figure S10. ESI-MS of $[PIMPS]_3PW_{12}O_{40}$.

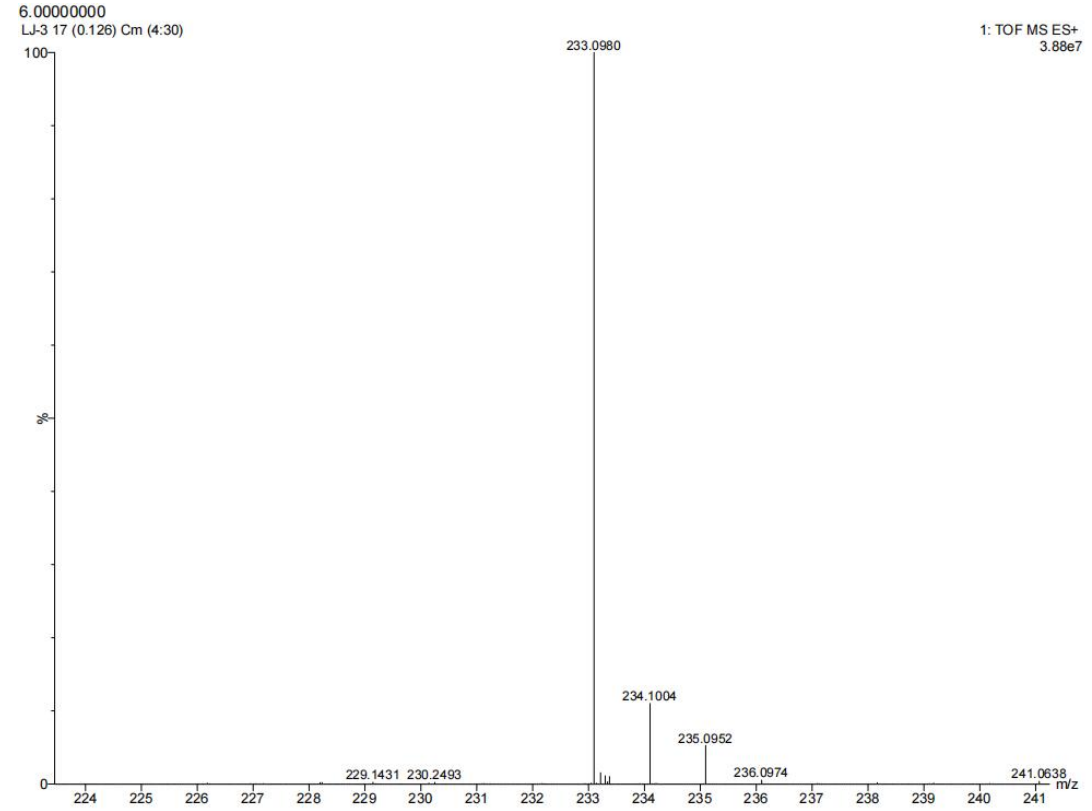

(a) Positive-ion ESI-MS of $[PIMPS]_3PW_{12}O_{40}$.

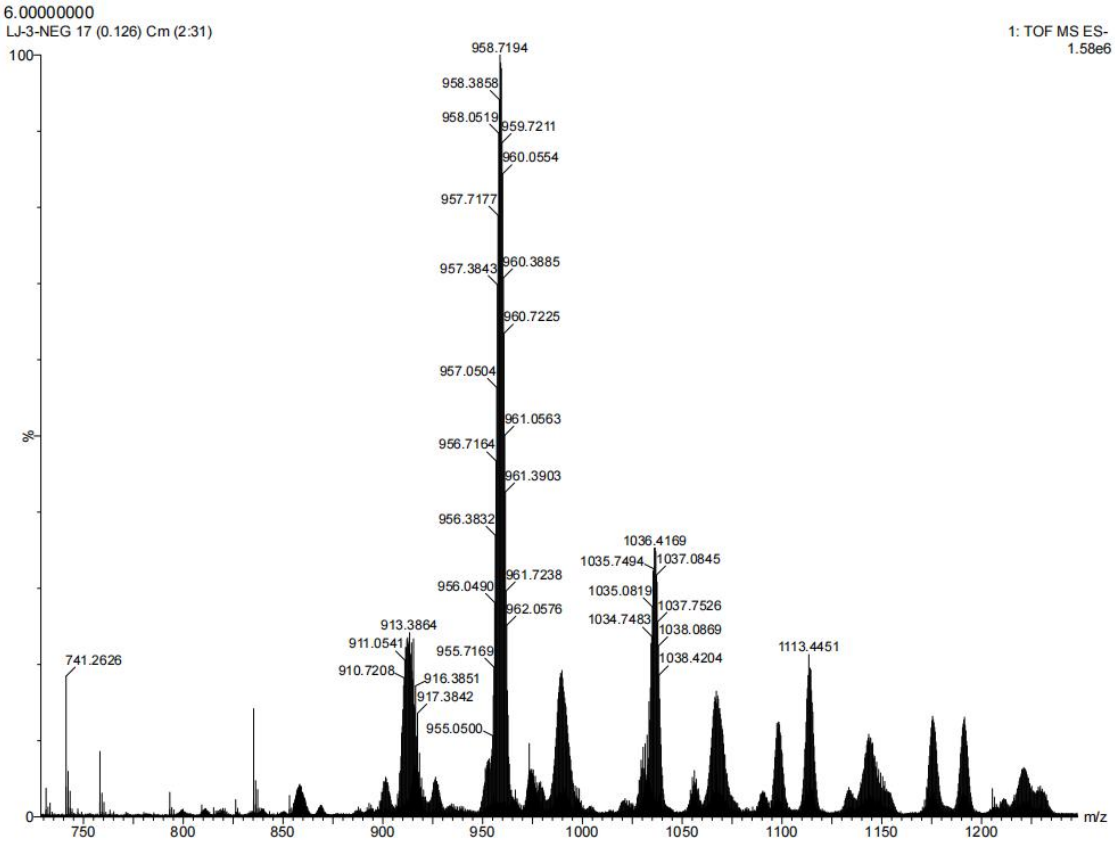

(b) Negative-ion ESI-MS of $[PIMPS]_3PW_{12}O_{40}$.

Figure S11. PXRD patterns of $[MIMPS]_3PW_{12}O_{40}$.

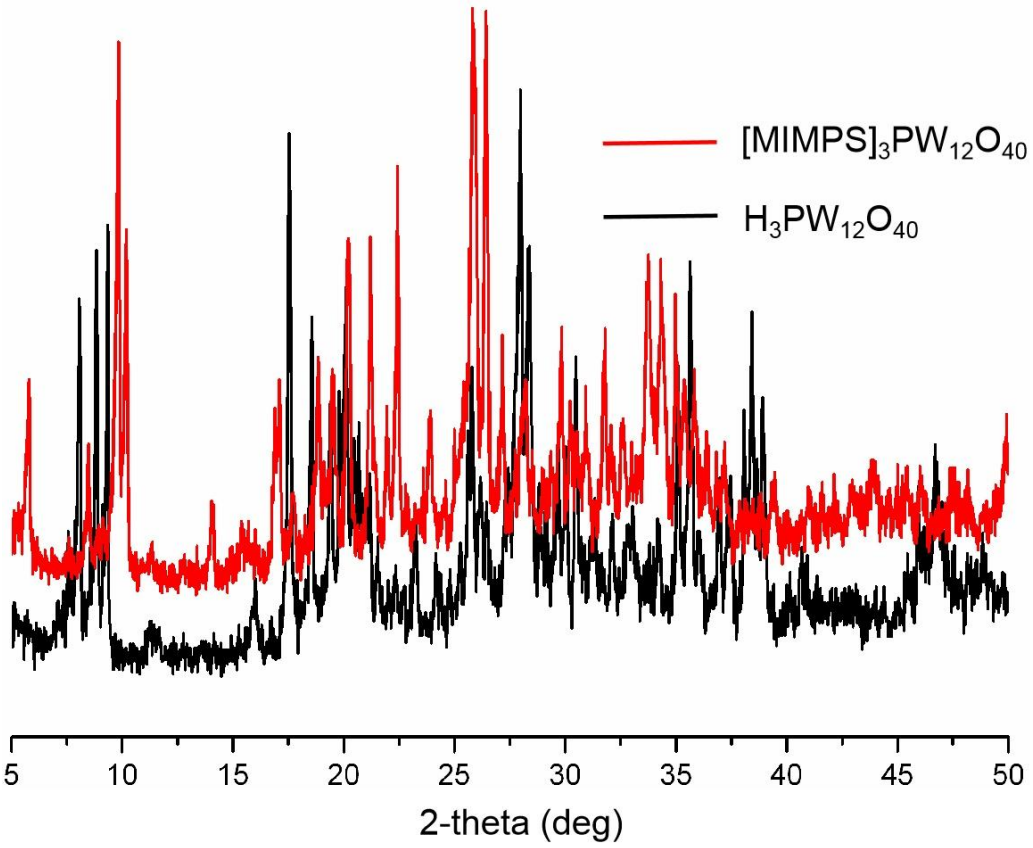

Figure S12. PXRD patterns of $[EIMPS]_3PW_{12}O_{40}$.

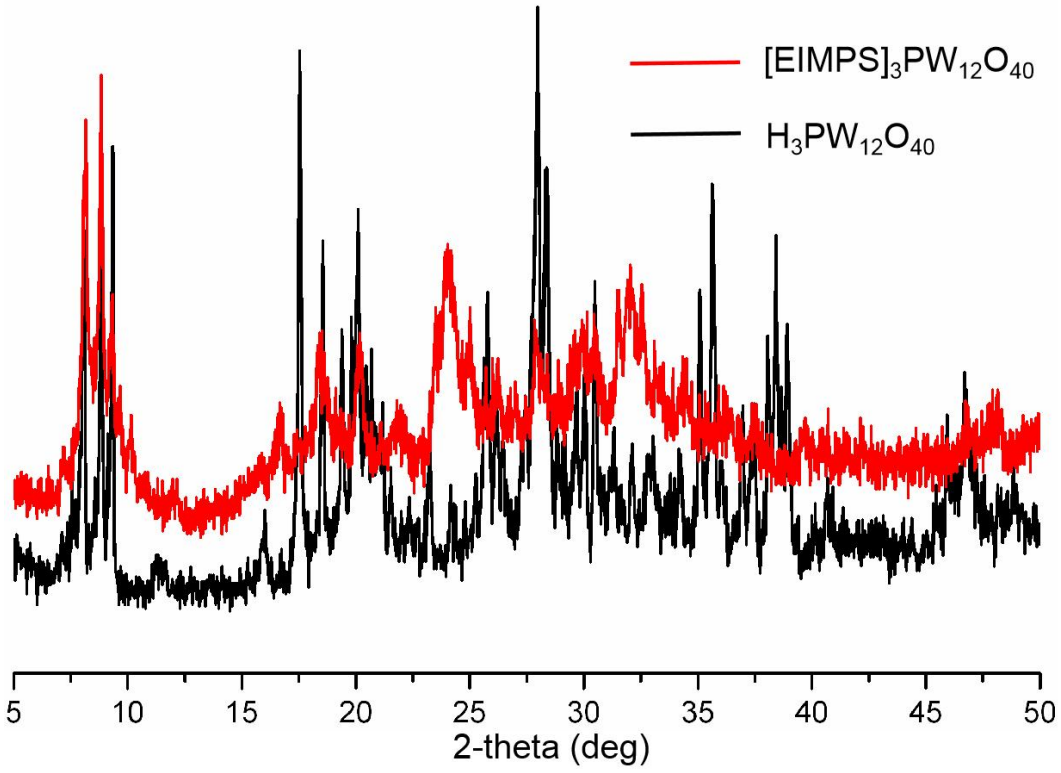

Figure S13. PXRD patterns of $[PIMPS]_3PW_{12}O_{40}$.

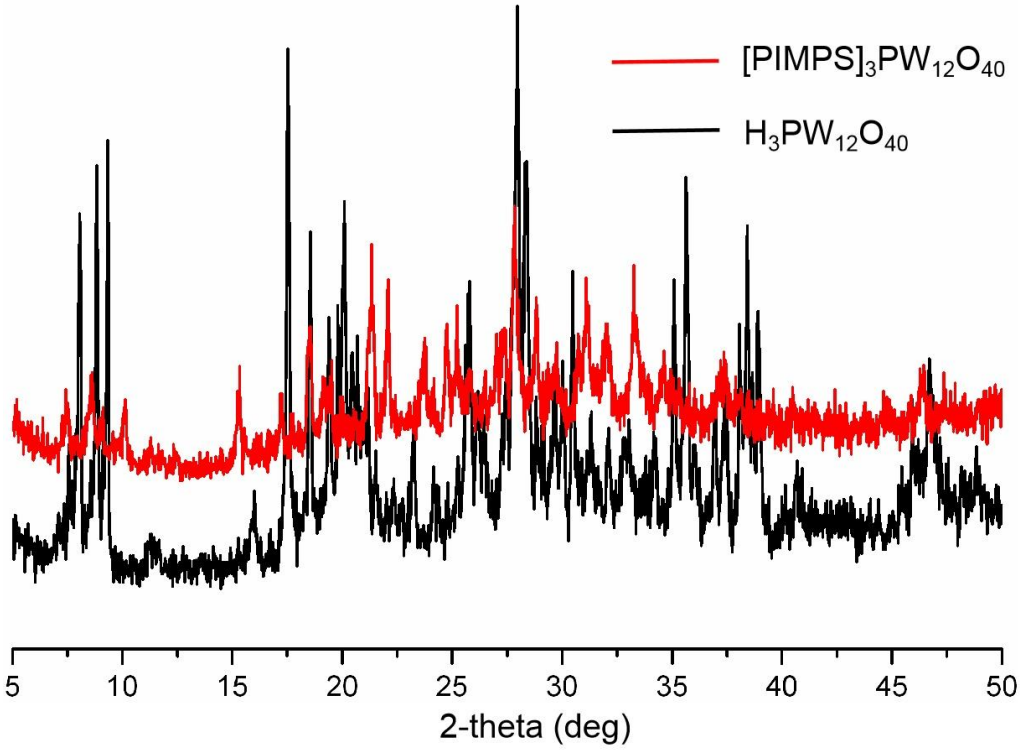

Figure S14. NMR spectra of (4-fluorophenyl)(2-phenylpropan-2-yl)sulfane.

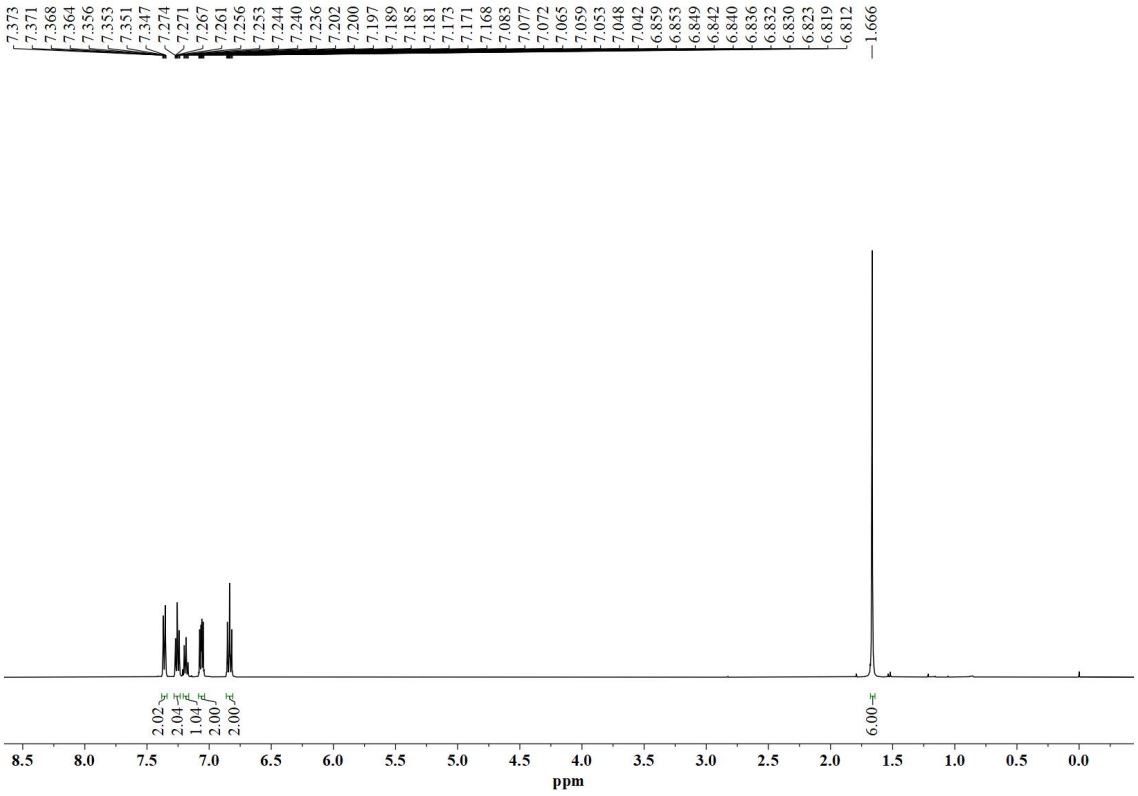

(a) ^1H NMR spectrum of (4-fluorophenyl)(2-phenylpropan-2-yl)sulfane in $CDCl_3$.

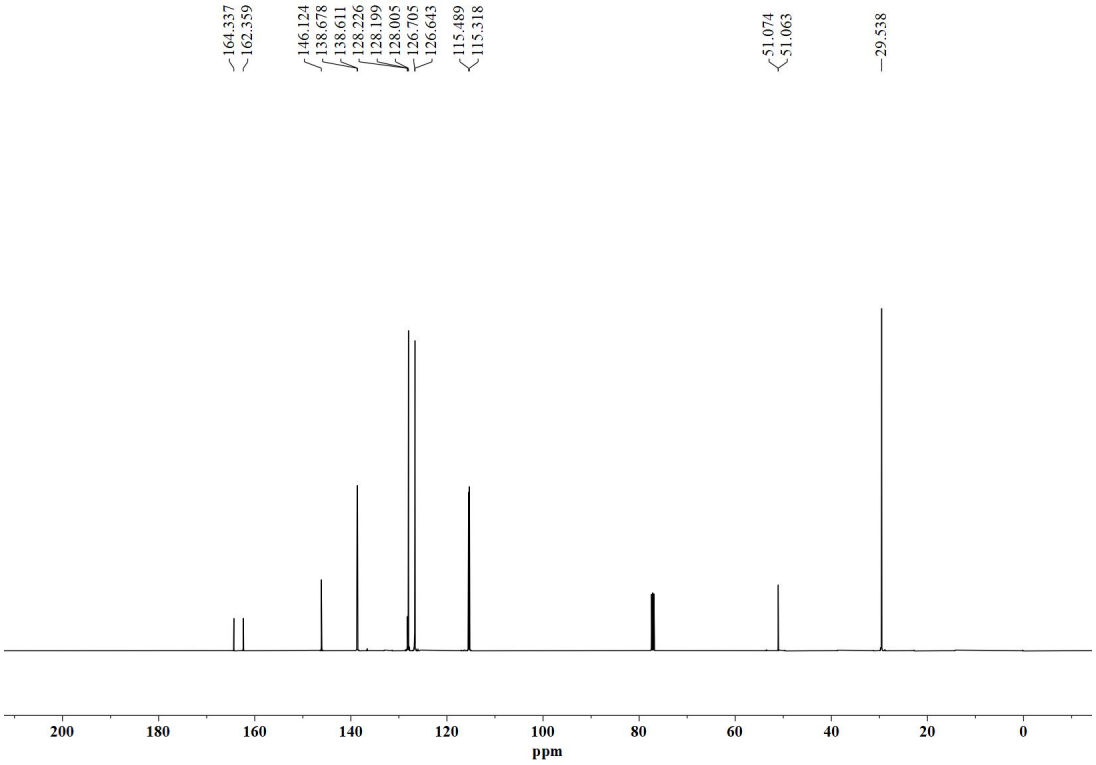

(b) ^{13}C NMR spectrum of (4-fluorophenyl)(2-phenylpropan-2-yl)sulfane in $CDCl_3$.

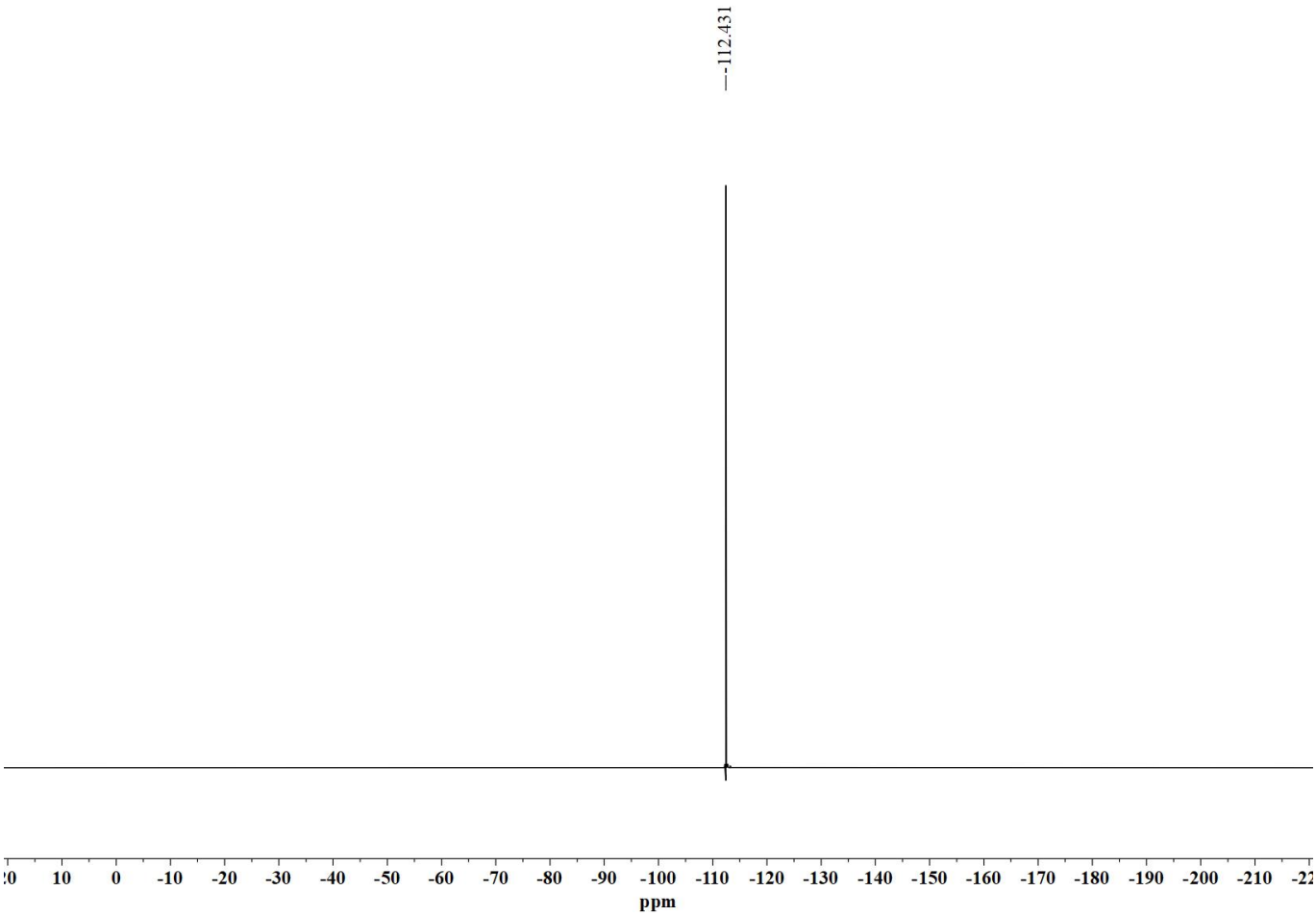

(c) ^{19}F NMR spectrum of (4-fluorophenyl)(2-phenylpropan-2-yl)sulfane in $CDCl_3$.

Figure S15. NMR spectra of (4-bromophenyl)(2-phenylpropan-2-yl)sulfane.

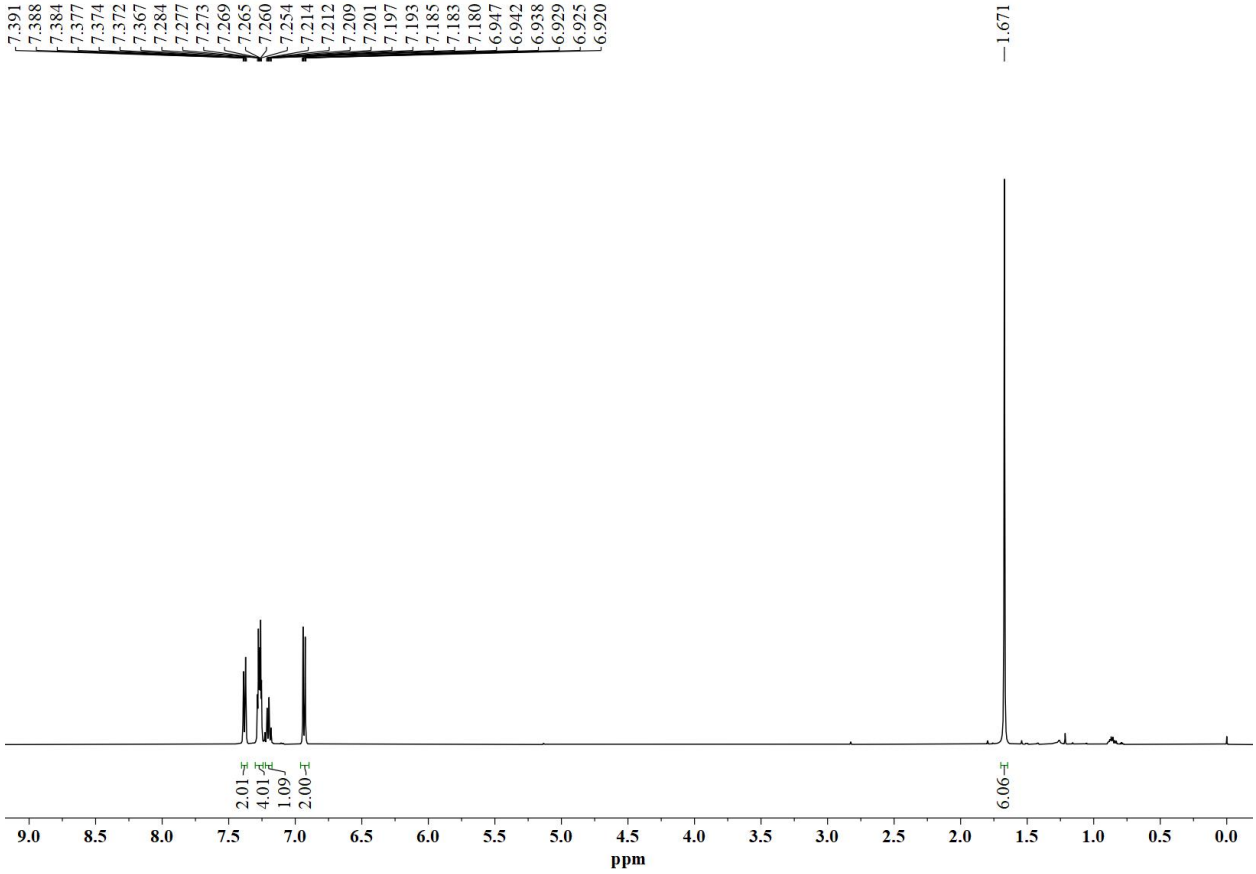

(a) ^{1}H NMR spectrum of (4-bromophenyl)(2-phenylpropan-2-yl)sulfane in $CDCl_3$.

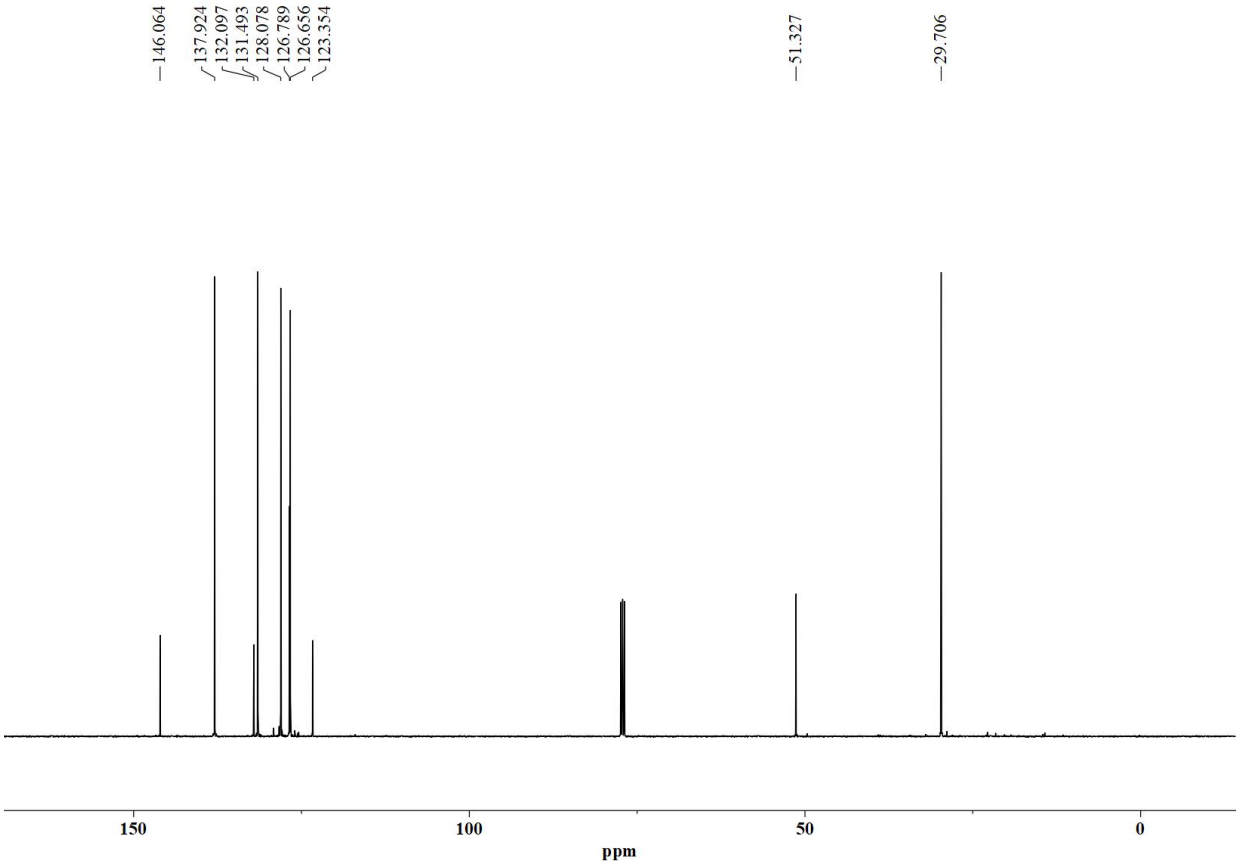

(b) ^{13}C NMR spectrum of (4-bromophenyl)(2-phenylpropan-2-yl)sulfane in $CDCl_3$.

Figure S16. NMR spectra of (4-chlorophenyl)(2-phenylpropan-2-yl)sulfane.

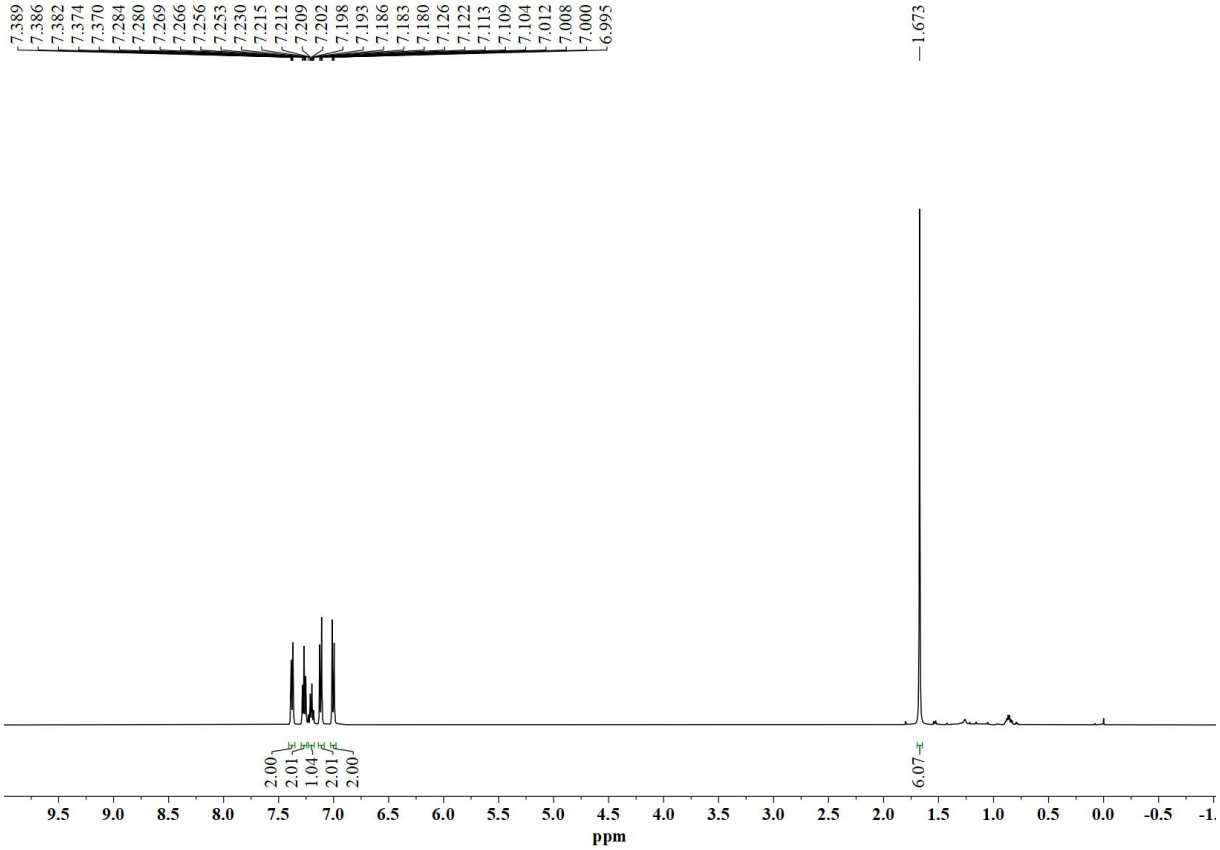

(a) ^{1}H NMR spectrum of (4-chlorophenyl)(2-phenylpropan-2-yl)sulfane in $CDCl_3$.

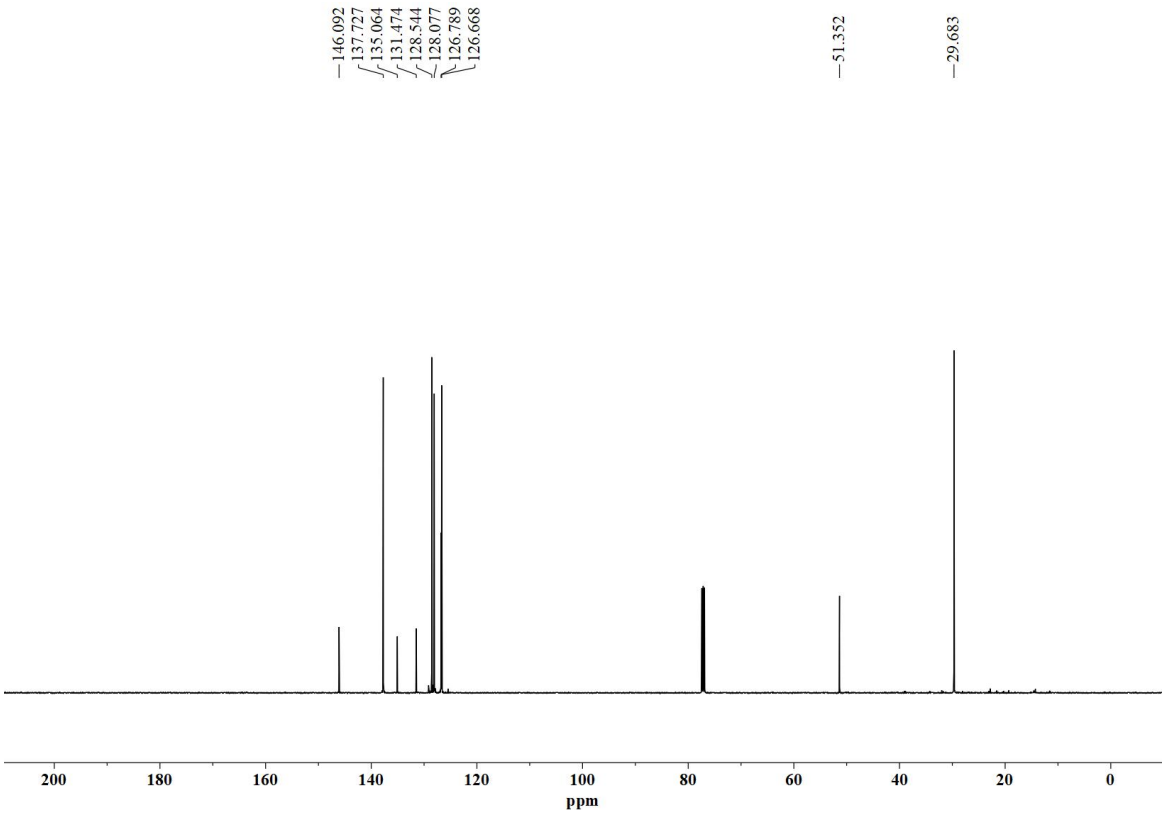

(b) ^{13}C NMR spectrum of (4-chlorophenyl)(2-phenylpropan-2-yl)sulfane in $CDCl_3$.

Figure S17. NMR spectra of (3-chlorophenyl)(2-phenylpropan-2-yl)sulfane.

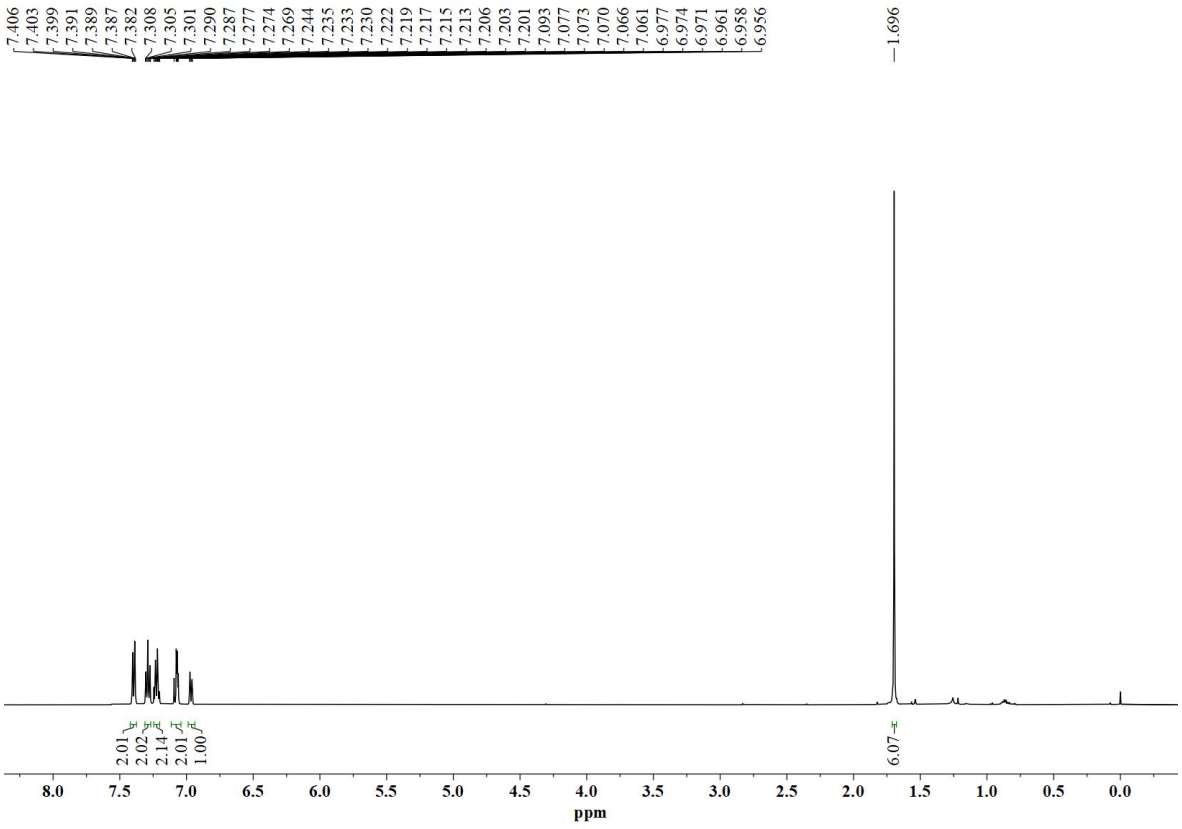

(a) ^{1}H NMR spectrum of (3-chlorophenyl)(2-phenylpropan-2-yl)sulfane in $CDCl_3$.

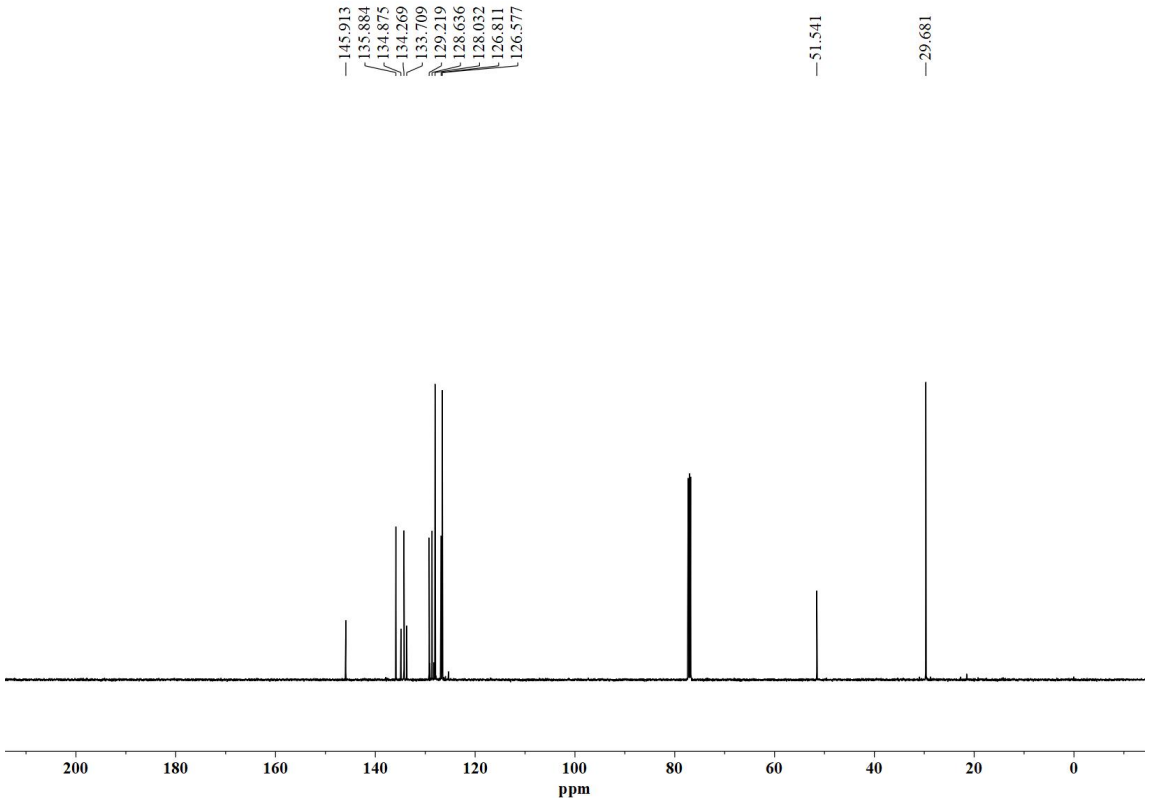

(b) ^{13}C NMR spectrum of (3-chlorophenyl)(2-phenylpropan-2-yl)sulfane in $CDCl_3$.

Figure S18. NMR spectra of (2-chlorophenyl)(2-phenylpropan-2-yl)sulfane.

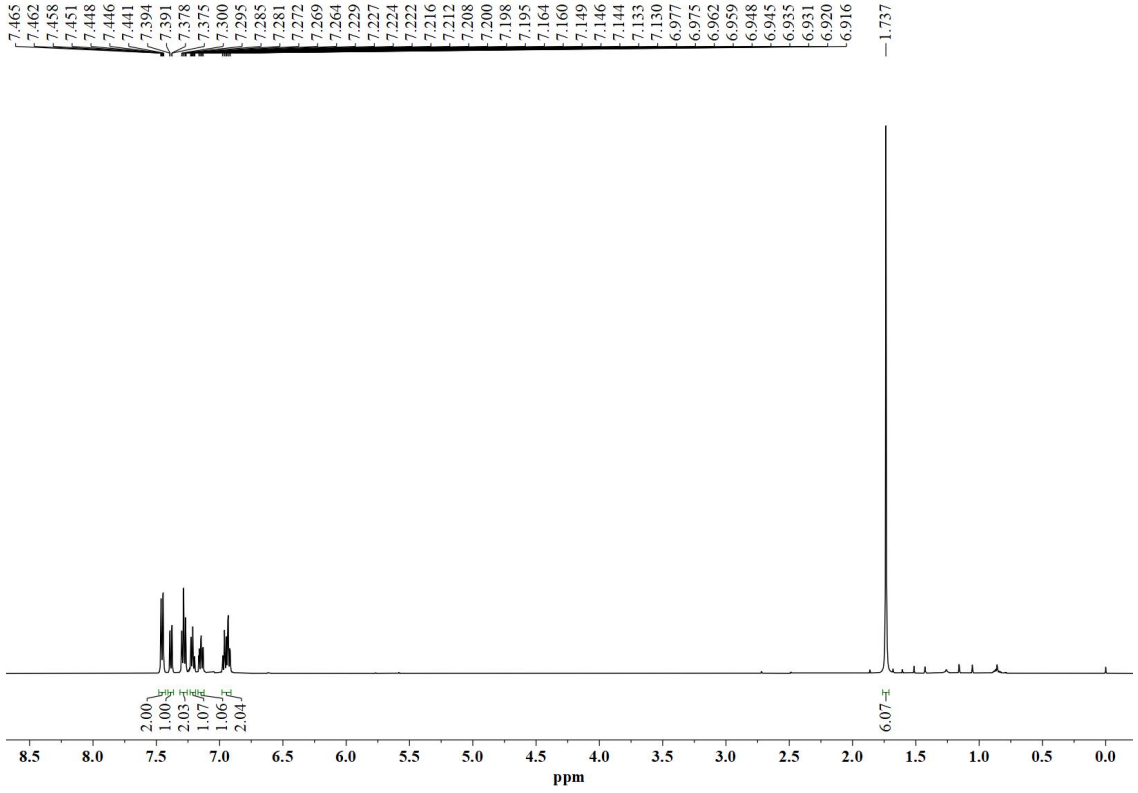

(a) ^{1}H NMR spectrum of (2-chlorophenyl)(2-phenylpropan-2-yl)sulfane in $CDCl_3$.

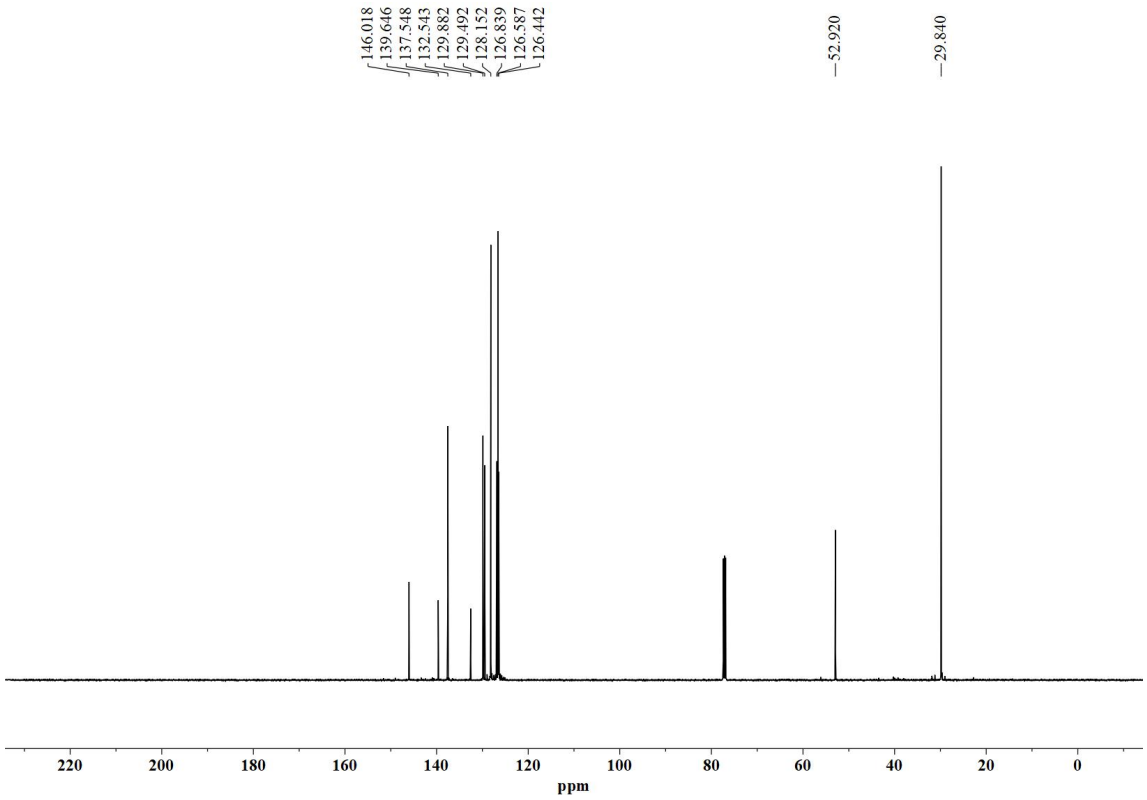

(b) ^{13}C NMR spectrum of (2-chlorophenyl)(2-phenylpropan-2-yl)sulfane in $CDCl_3$.

Figure S19. NMR spectra of (2-phenylpropan-2-yl)(p-tolyl)sulfane.

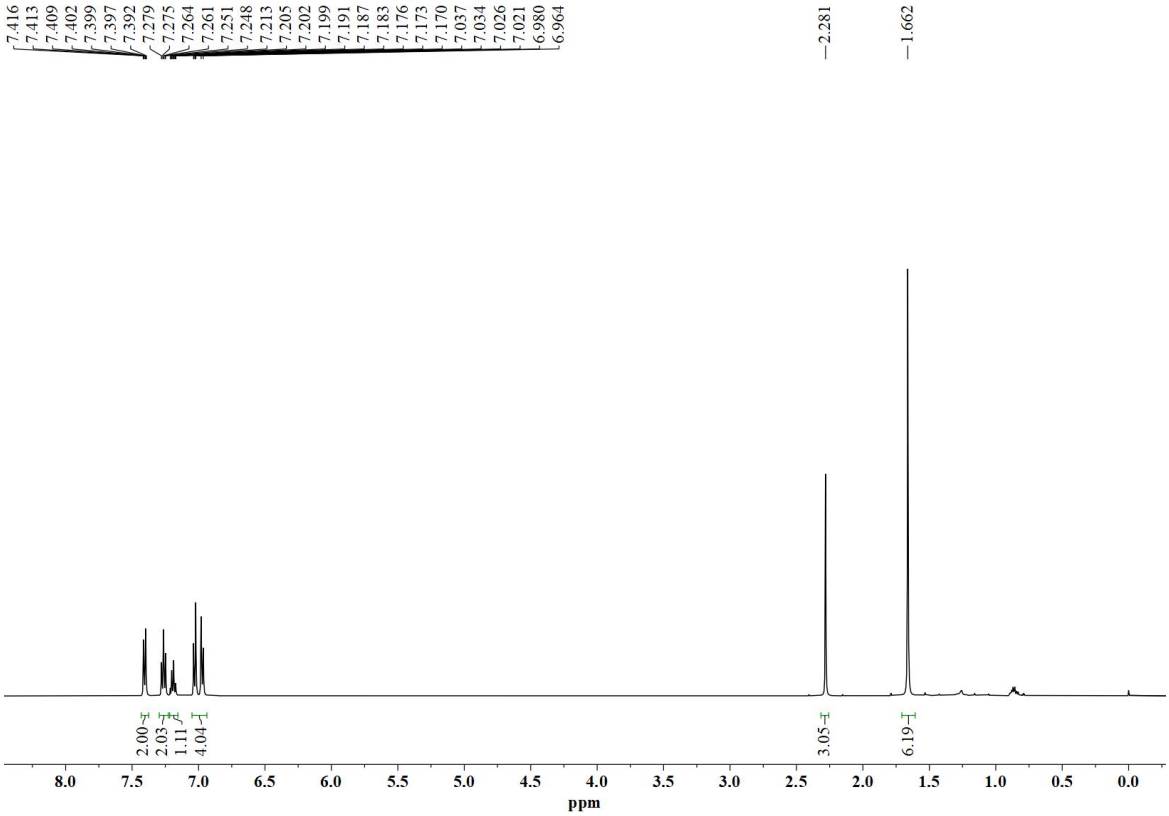

(a) ^{1}H NMR spectrum of (2-phenylpropan-2-yl)(p-tolyl)sulfane in $CDCl_3$.

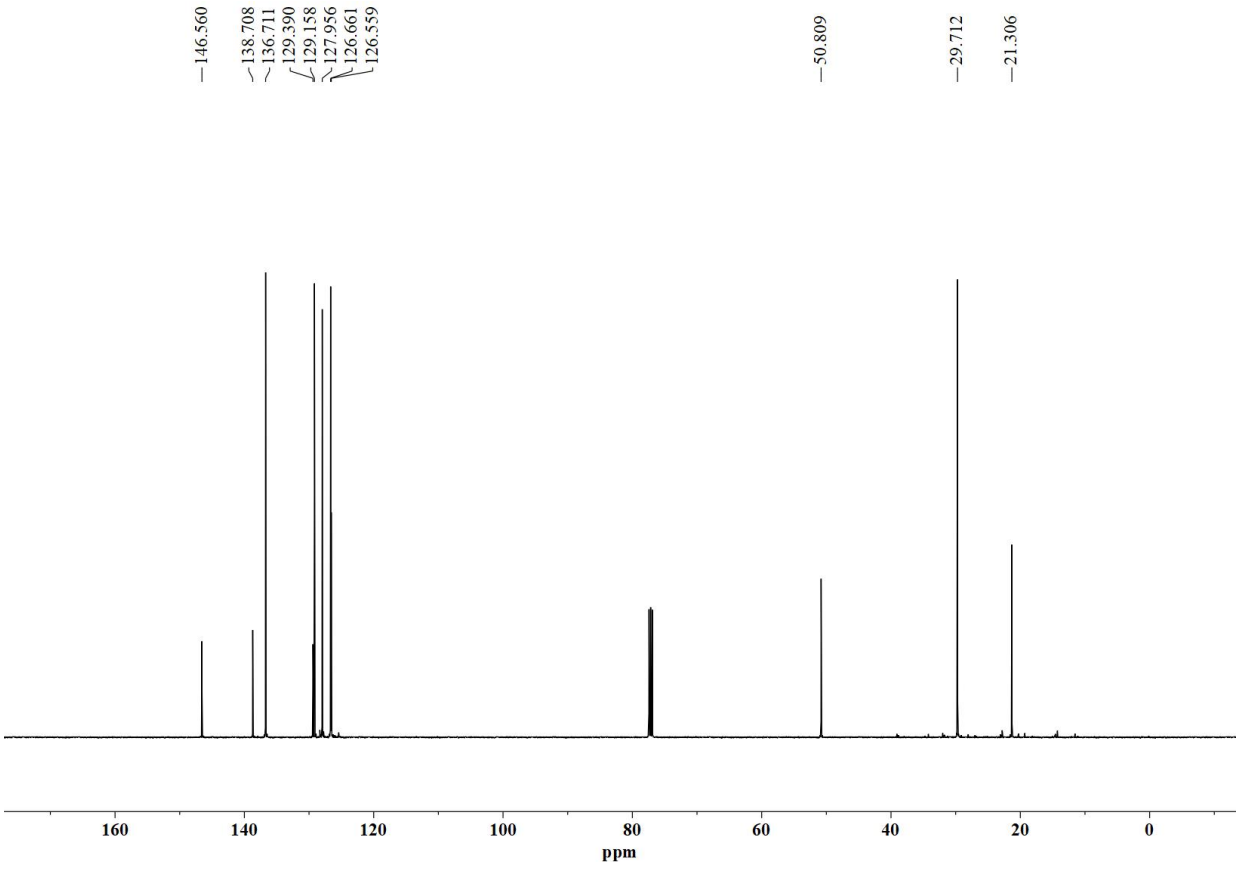

(b) ^{13}C NMR spectrum of (2-phenylpropan-2-yl)(p-tolyl)sulfane in $CDCl_3$.

Figure S20. NMR spectra of (4-methoxyphenyl)(2-phenylpropan-2-yl)sulfane.

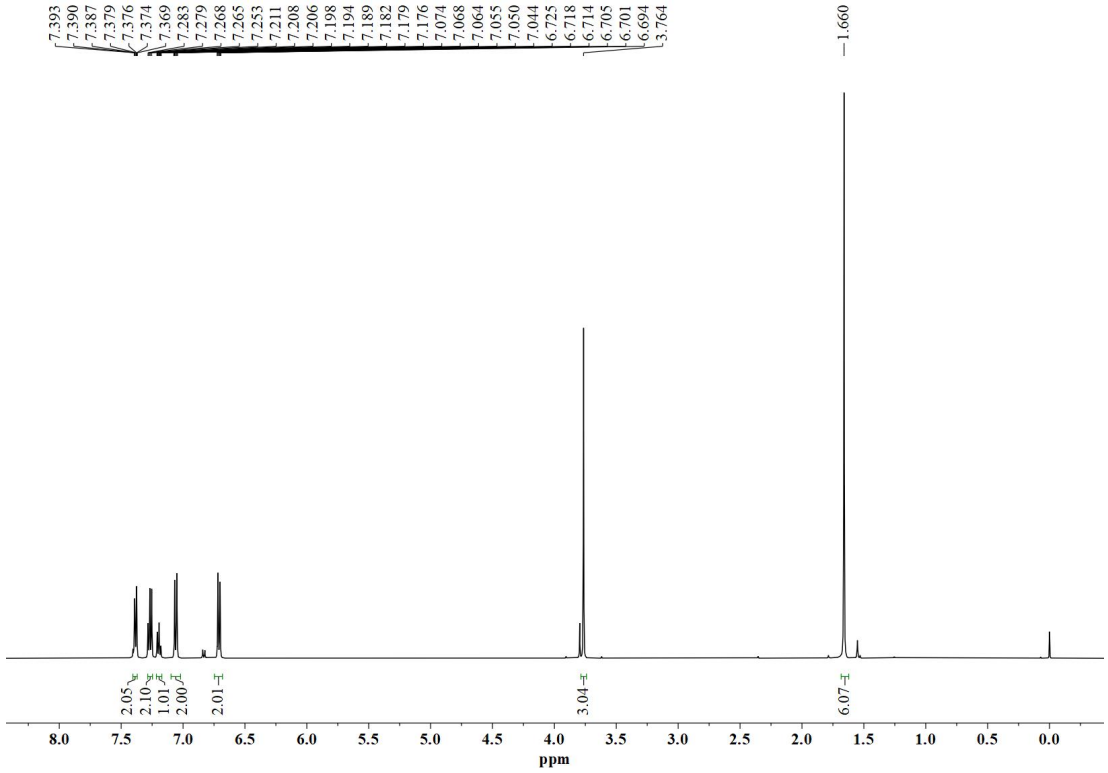

(a) ^{1}H NMR spectrum of (4-methoxyphenyl)(2-phenylpropan-2-yl)sulfane in $CDCl_3$.

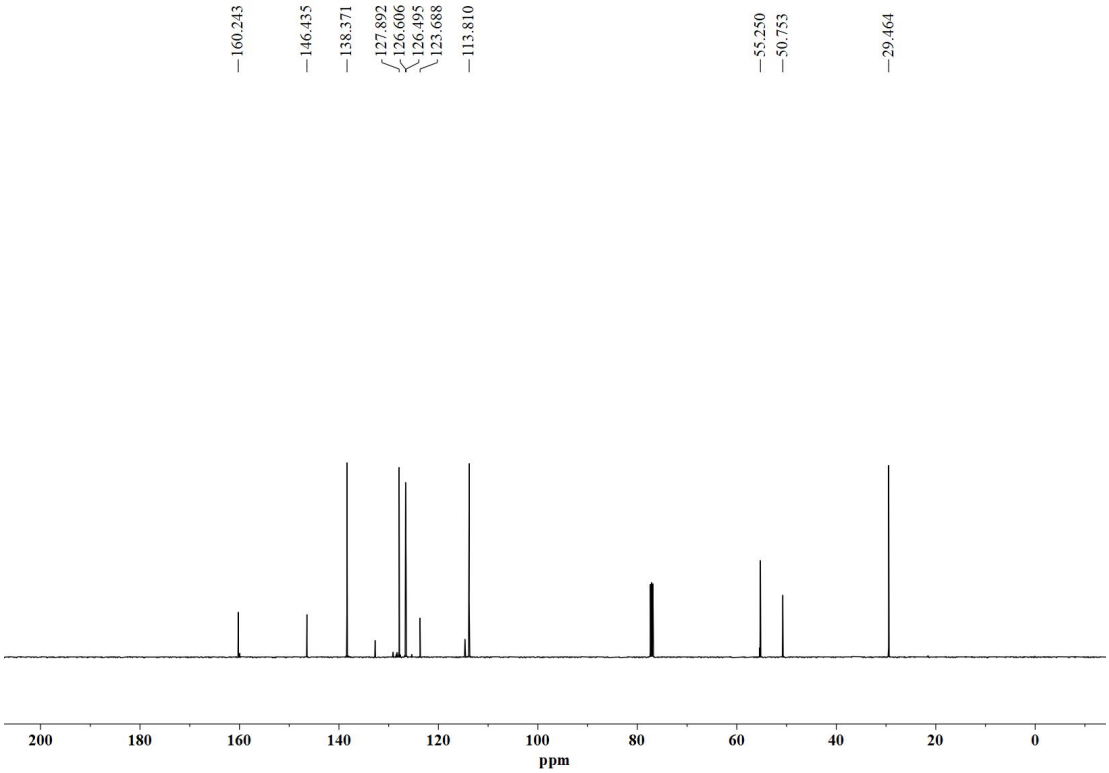

(b) ^{13}C NMR spectrum of (4-methoxyphenyl)(2-phenylpropan-2-yl)sulfane in $CDCl_3$.

Figure S21. NMR spectra of cyclopentyl(2-phenylpropan-2-yl)sulfane.

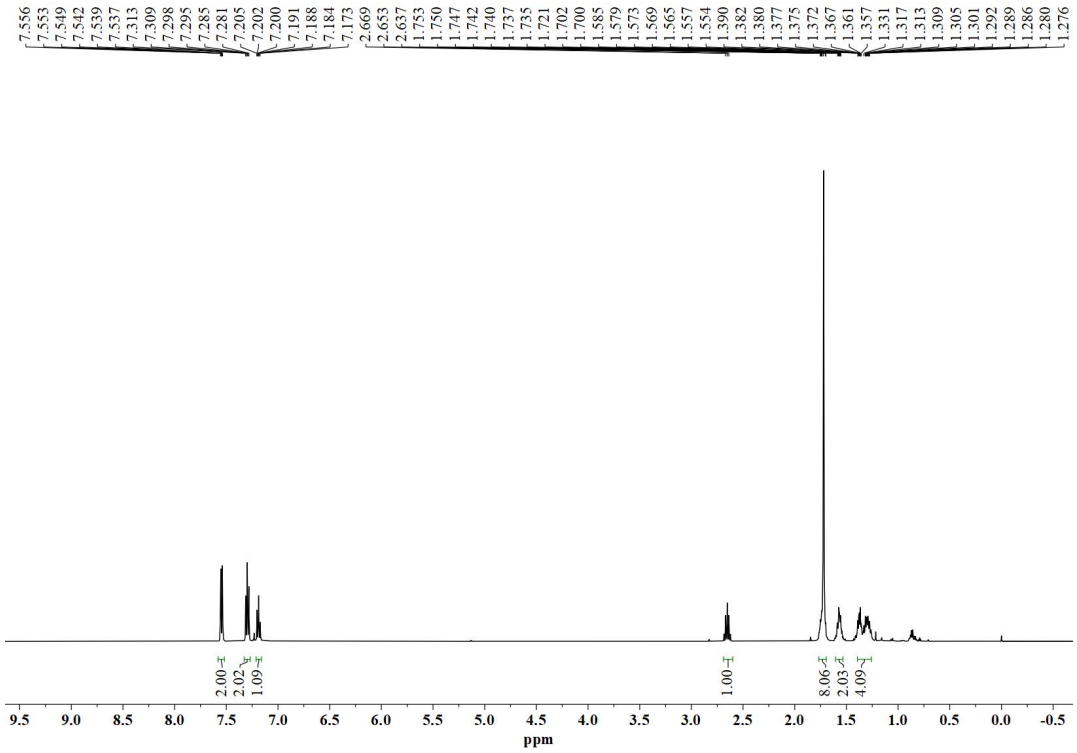

(a) ^{1}H NMR spectrum of cyclopentyl(2-phenylpropan-2-yl)sulfane in $CDCl_3$.

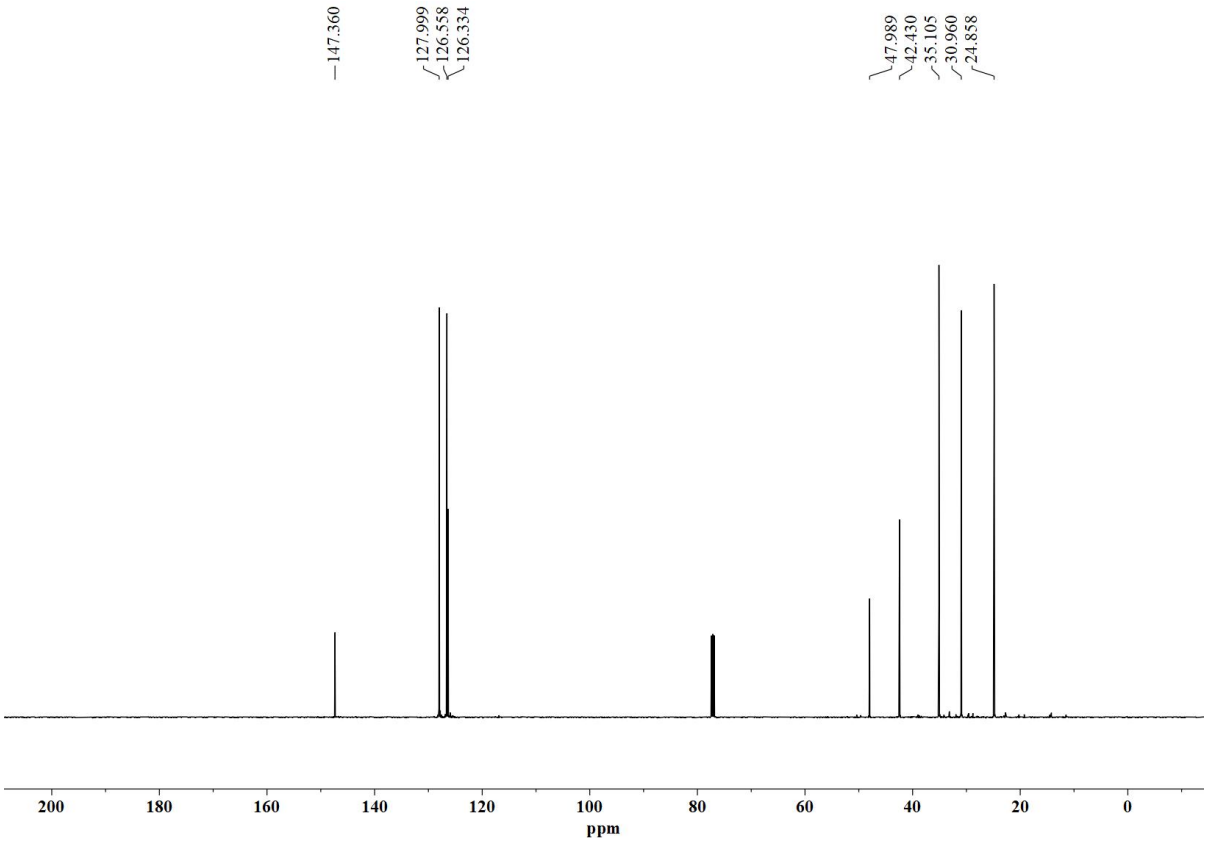

(b) ^{13}C NMR spectrum of cyclopentyl(2-phenylpropan-2-yl)sulfane in $CDCl_3$.

Figure S22. NMR spectra of cyclohexyl(2-phenylpropan-2-yl)sulfane.

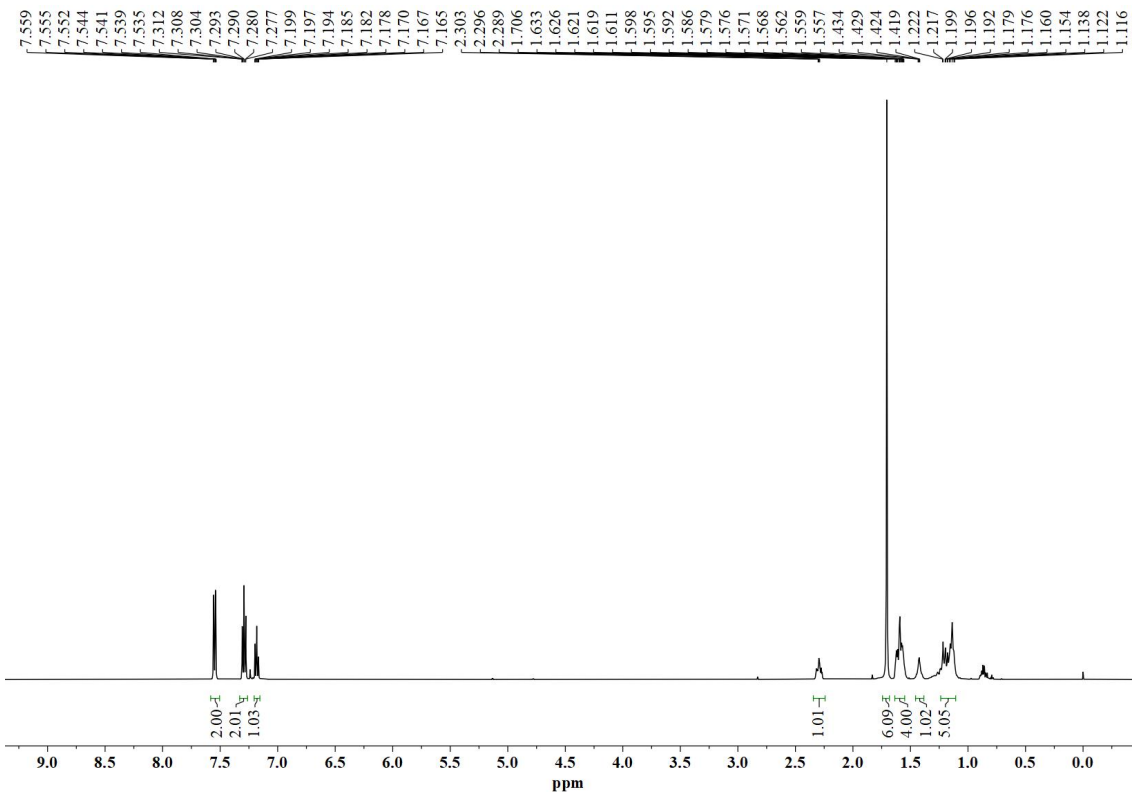

(a) ^{1}H NMR spectrum of cyclohexyl(2-phenylpropan-2-yl)sulfane in $CDCl_3$.

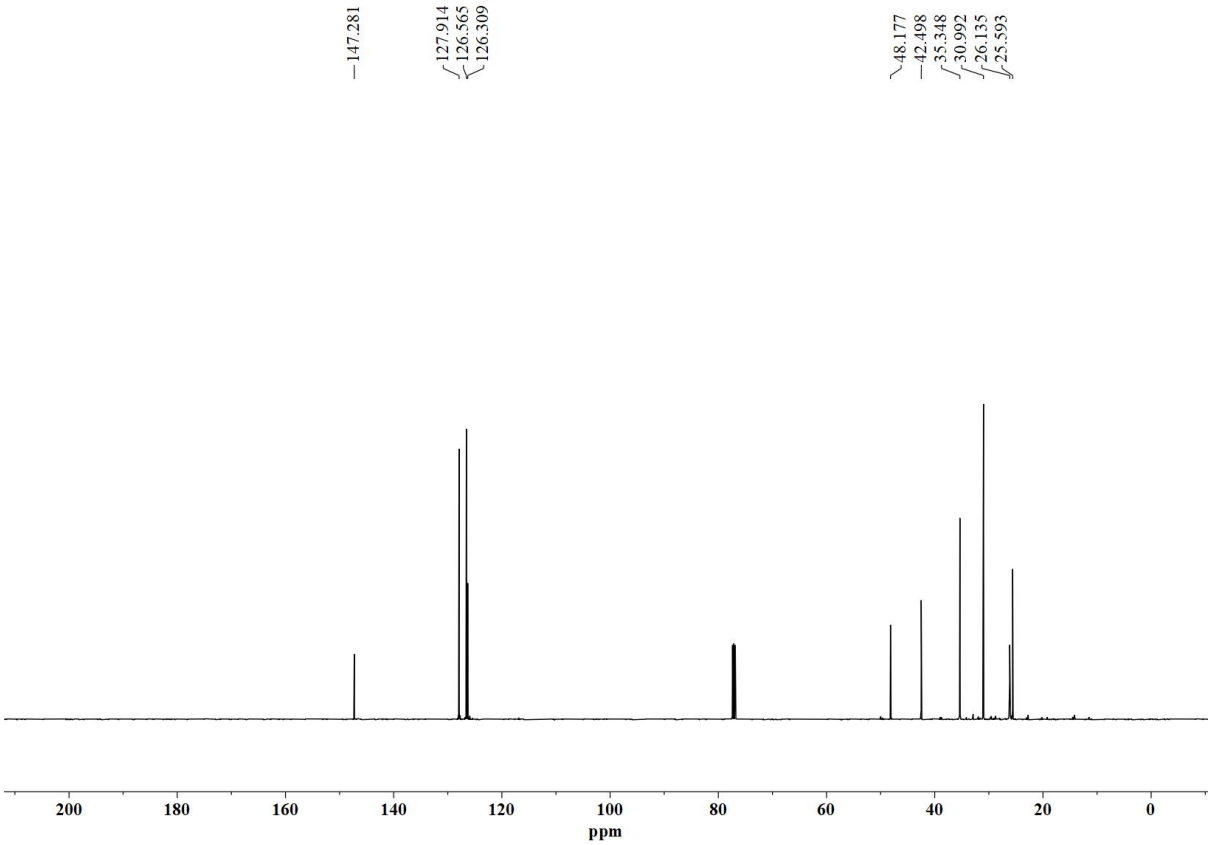

(b) ^{13}C NMR spectrum of cyclohexyl(2-phenylpropan-2-yl)sulfane in $CDCl_3$.

Figure S23. NMR spectra of (4-fluorophenyl)(1-phenylethyl)sulfane.

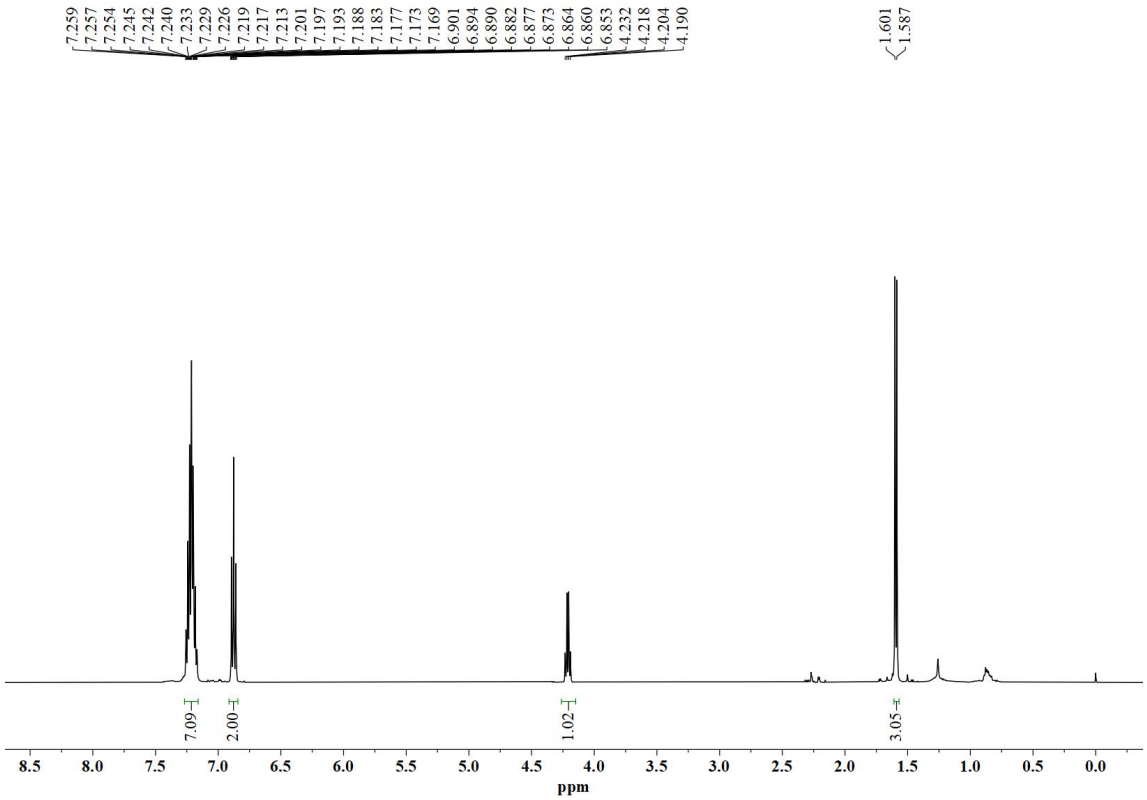

(a) ^{1}H NMR spectrum of (4-fluorophenyl)(1-phenylethyl)sulfane in $CDCl_3$.

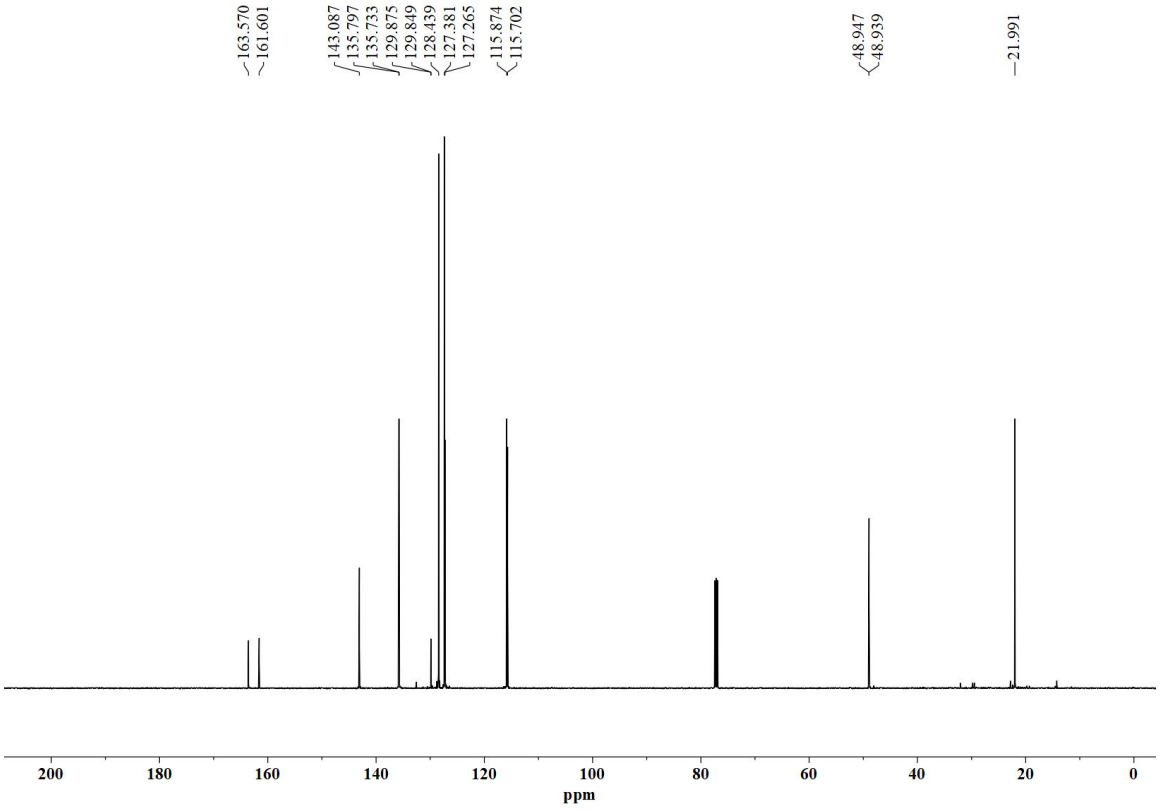

(b) ^{13}C NMR spectrum of (4-fluorophenyl)(1-phenylethyl)sulfane in $CDCl_3$.

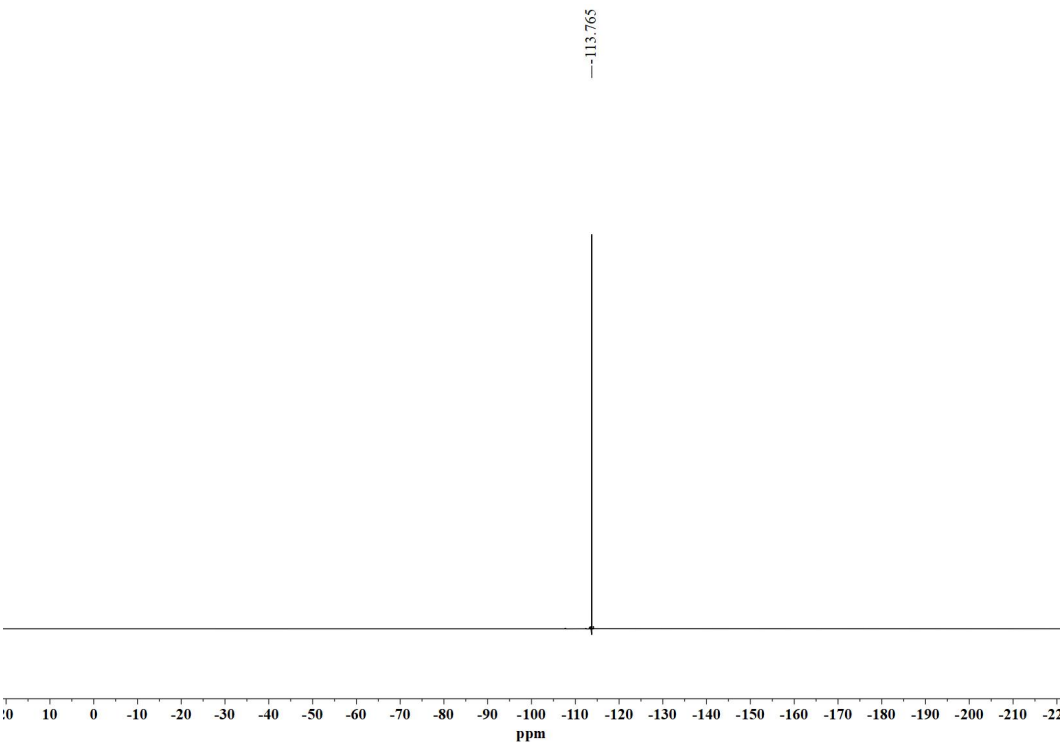

(c) ^{19}F NMR spectrum of (4-fluorophenyl)(1-phenylethyl)sulfane in $CDCl_3$.

Figure S24. NMR spectra of (4-bromophenyl)(1-phenylethyl)sulfane.

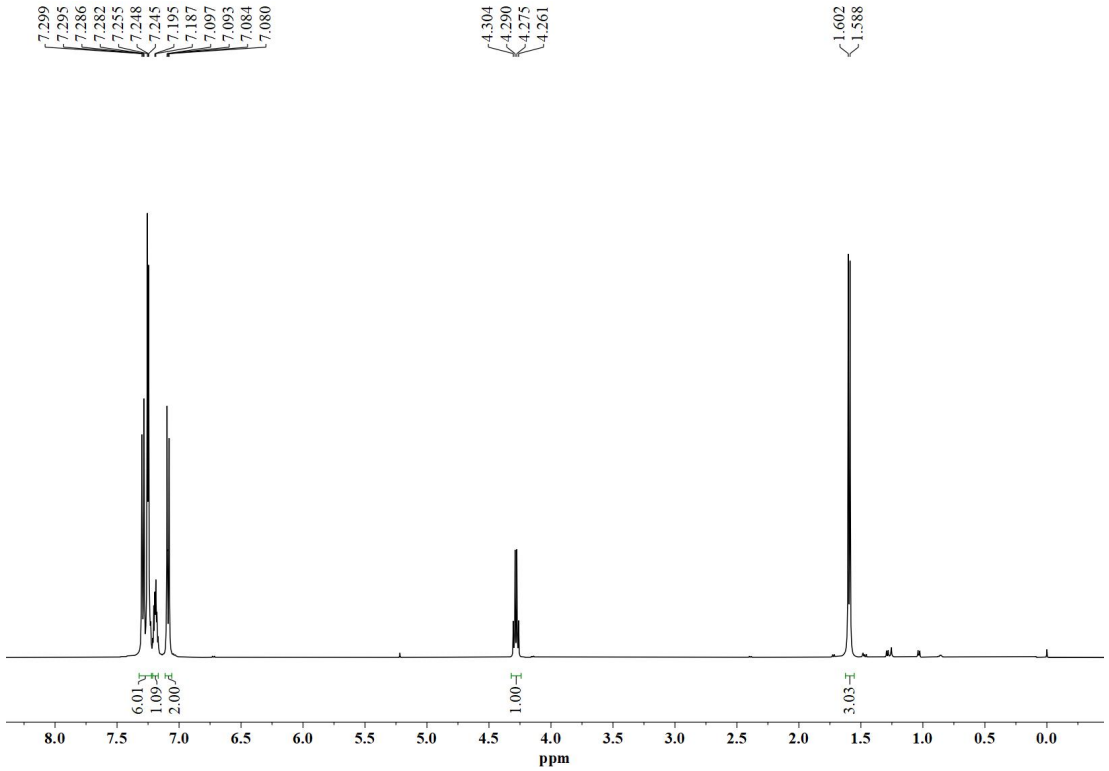

(a) ^{1}H NMR spectrum of (4-bromophenyl)(1-phenylethyl)sulfane in $CDCl_3$.

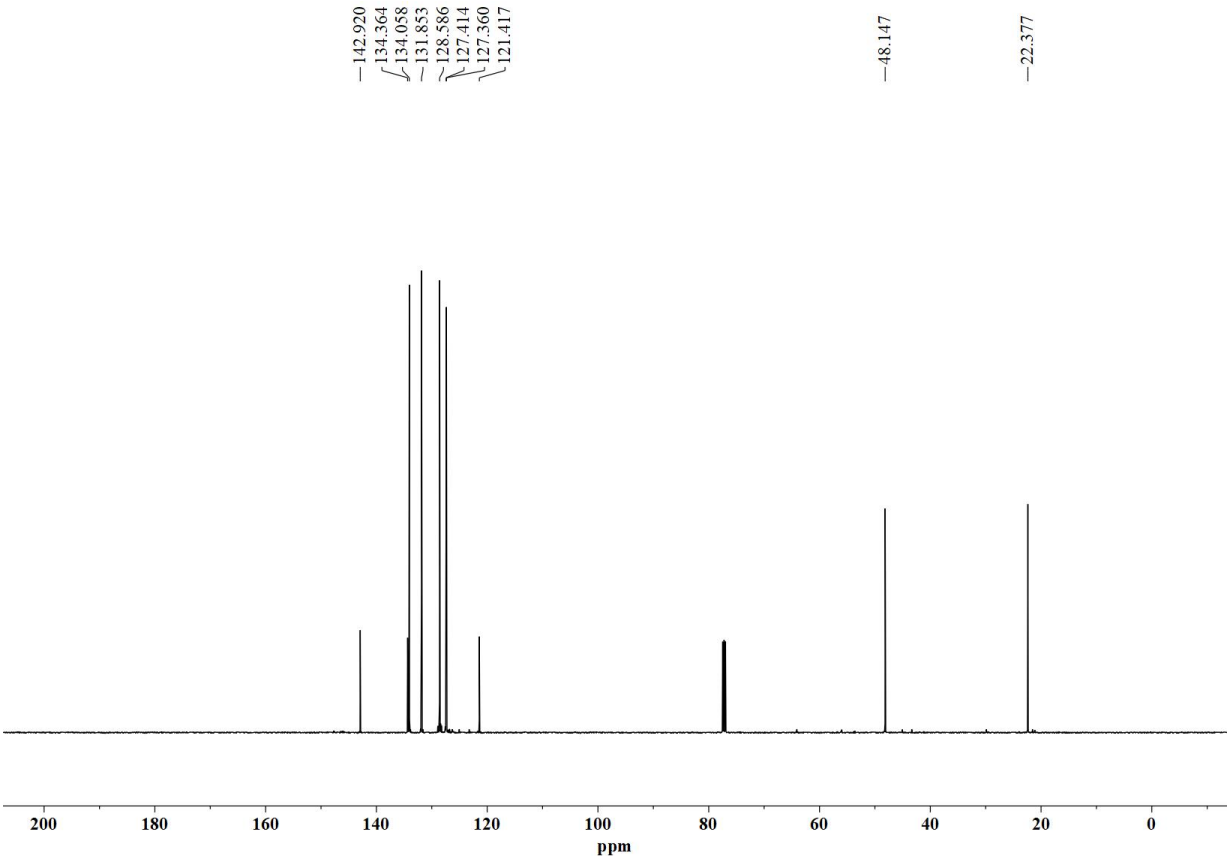

(b) ^{13}C NMR spectrum of (4-bromophenyl)(1-phenylethyl)sulfane in $CDCl_3$.

Figure S25. NMR spectra of (4-chlorophenyl)(1-phenylethyl)sulfane.

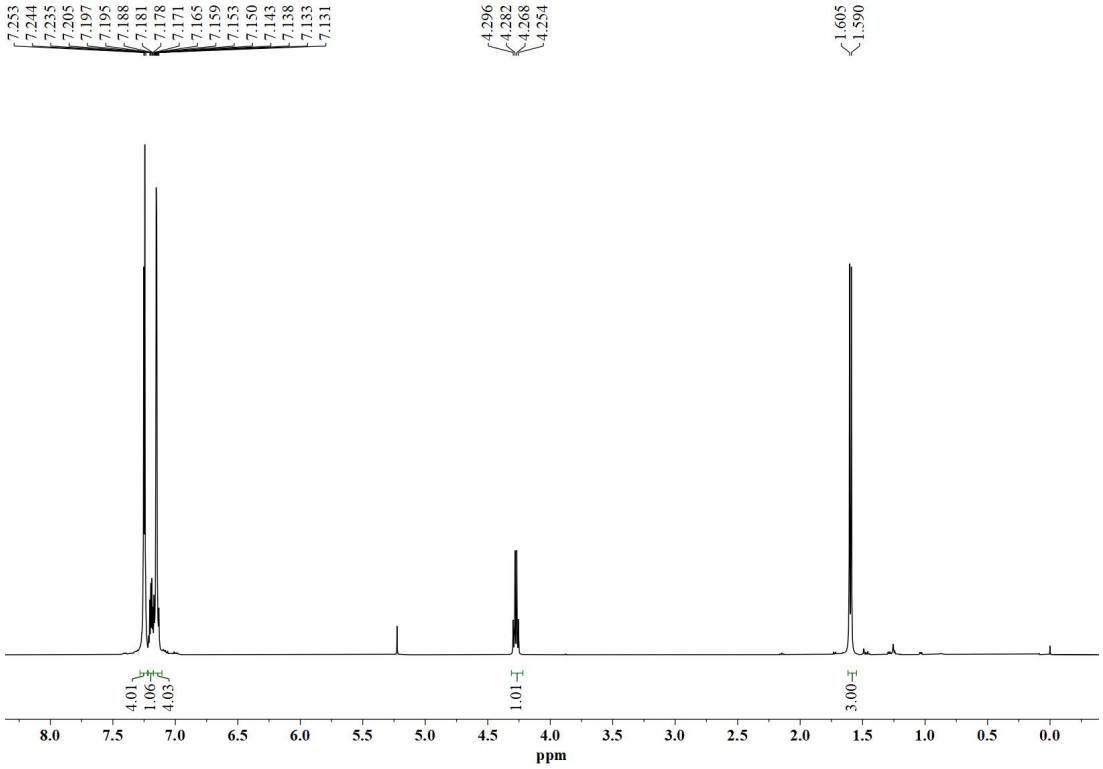

(a) ^{1}H NMR spectrum of (4-chlorophenyl)(1-phenylethyl)sulfane in $CDCl_3$.

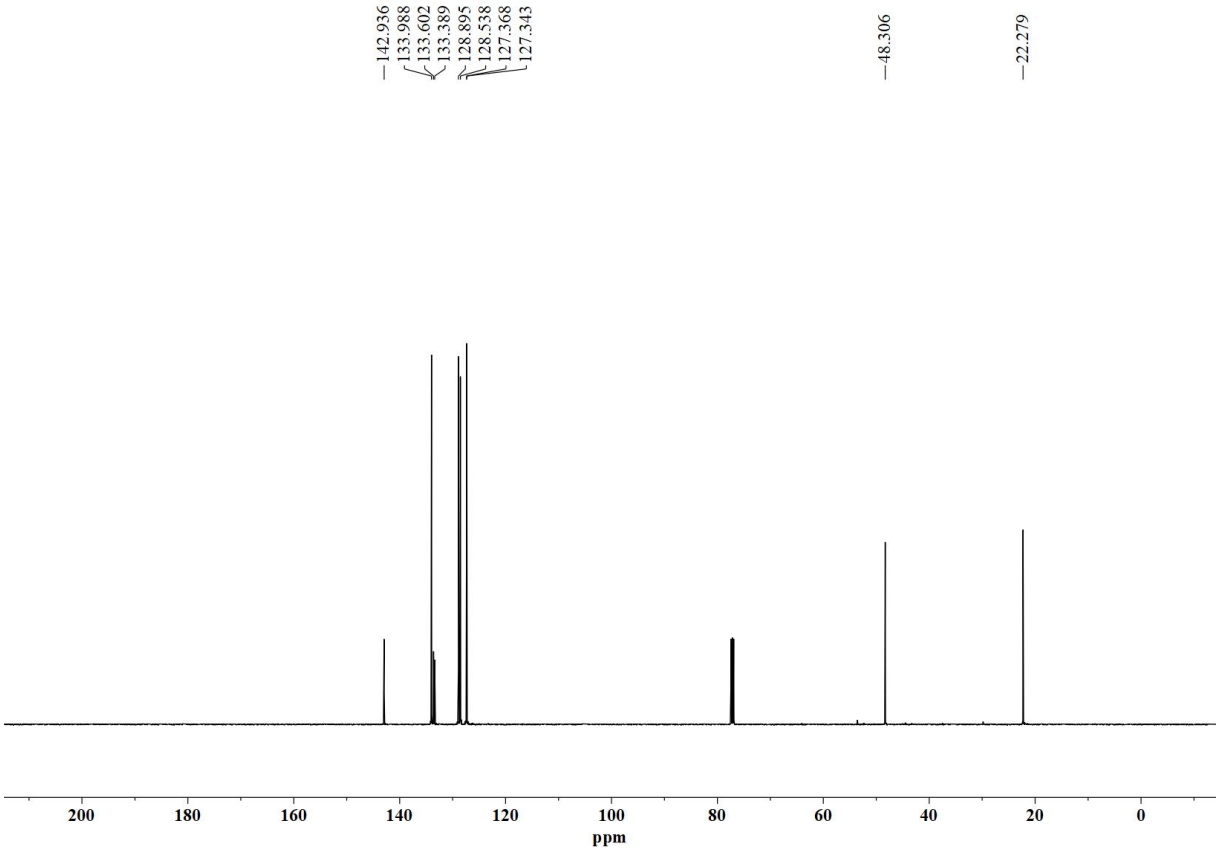

(b) ^{13}C NMR spectrum of (4-chlorophenyl)(1-phenylethyl)sulfane in $CDCl_3$.

Figure S26. NMR spectra of (3-chlorophenyl)(1-phenylethyl)sulfane.

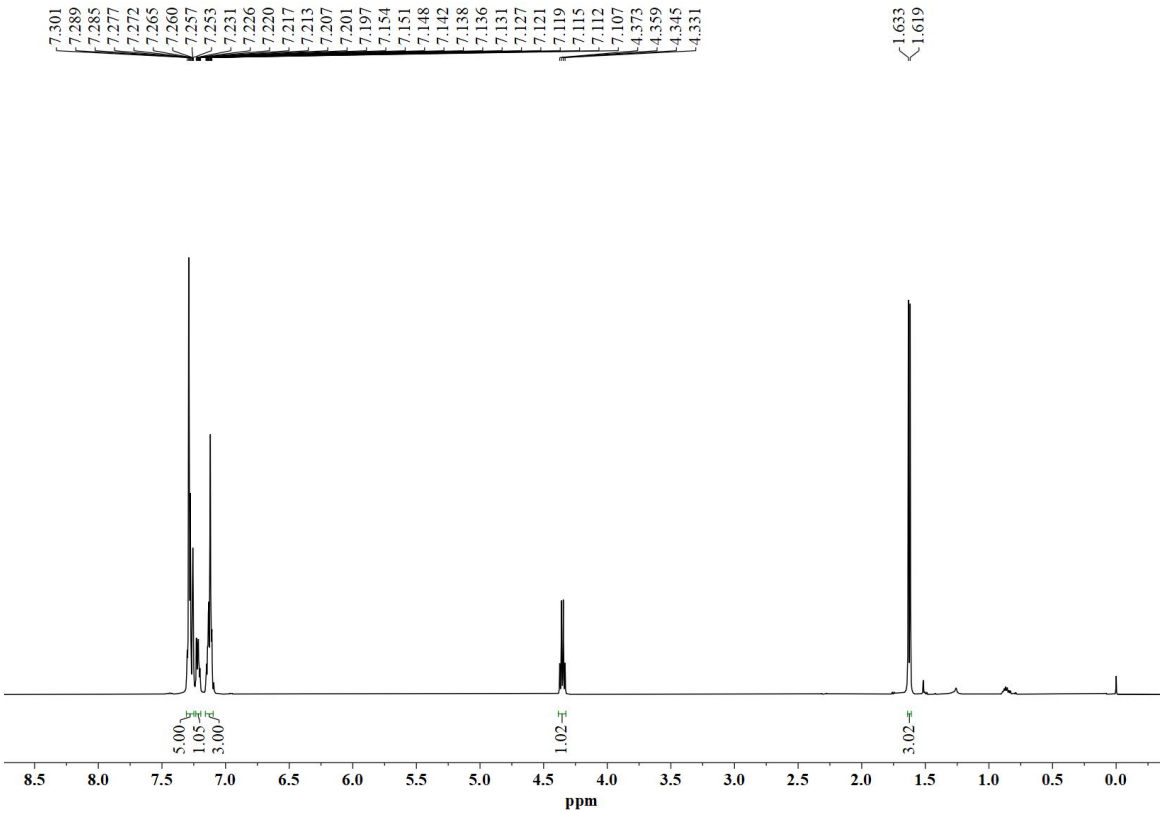

(a) ^{1}H NMR spectrum of (3-chlorophenyl)(1-phenylethyl)sulfane in $CDCl_3$.

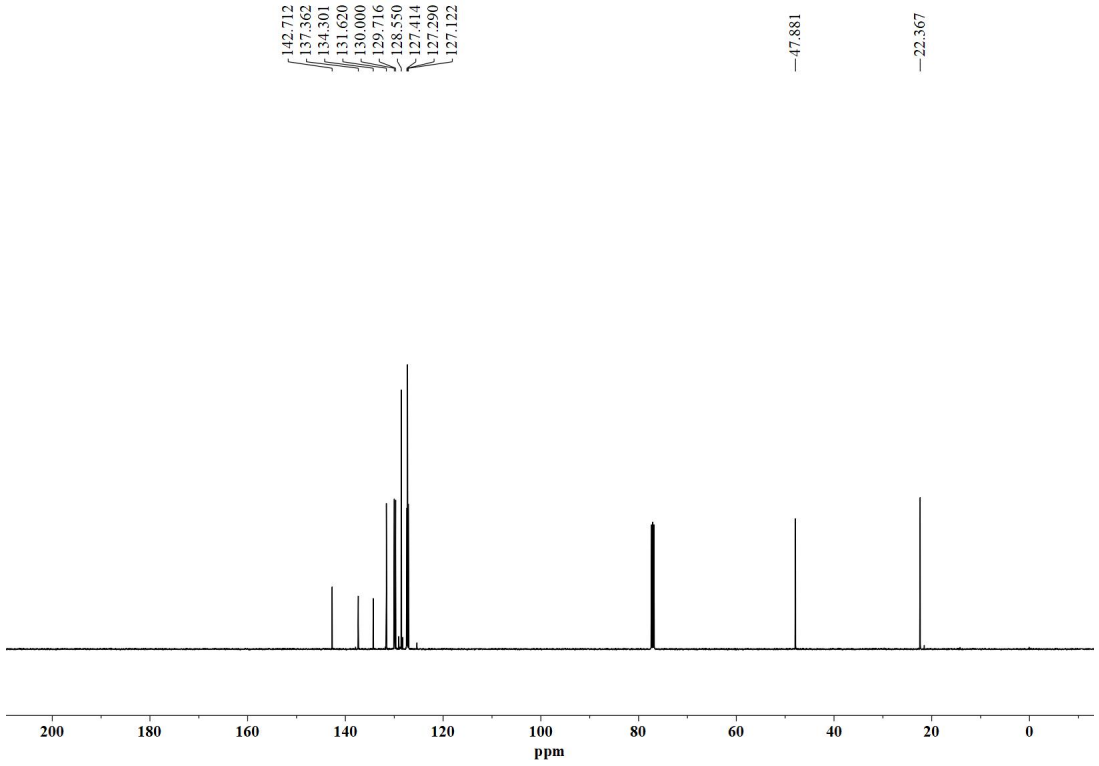

(b) ^{13}C NMR spectrum of (3-chlorophenyl)(1-phenylethyl)sulfane in $CDCl_3$.

Figure S27. NMR spectra of (2-chlorophenyl)(1-phenylethyl)sulfane.

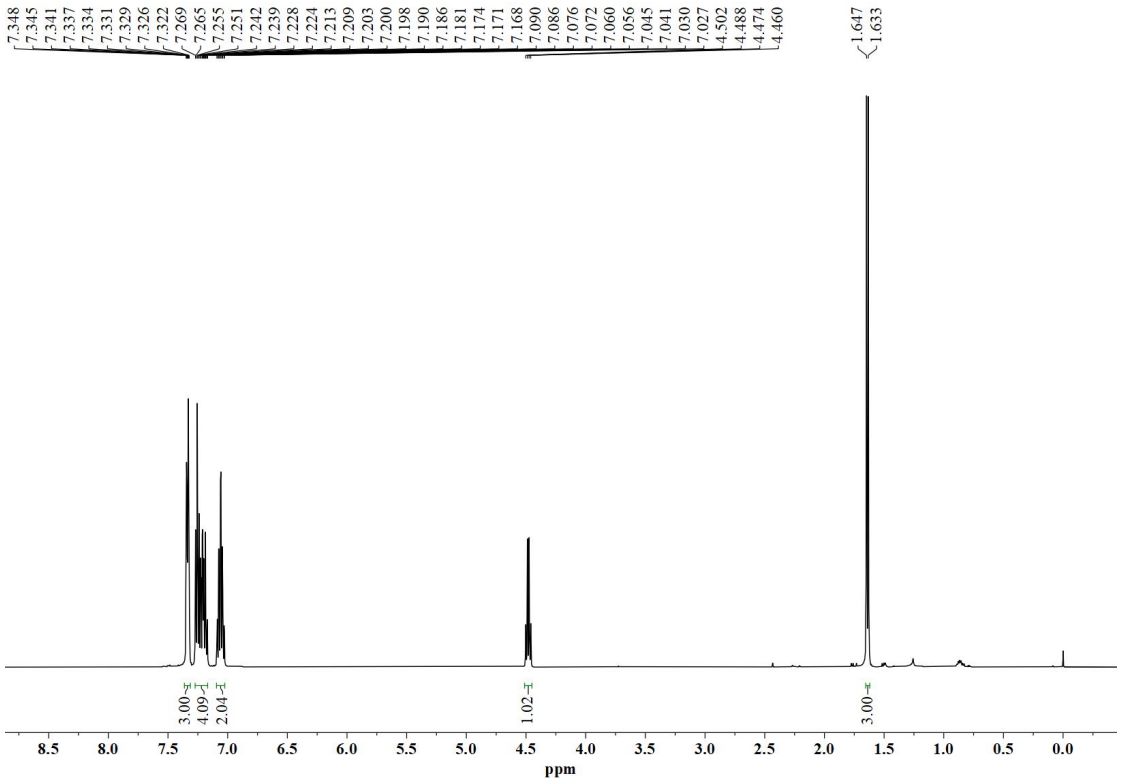

(a) ^{1}H NMR spectrum of (2-chlorophenyl)(1-phenylethyl)sulfane in $CDCl_3$.

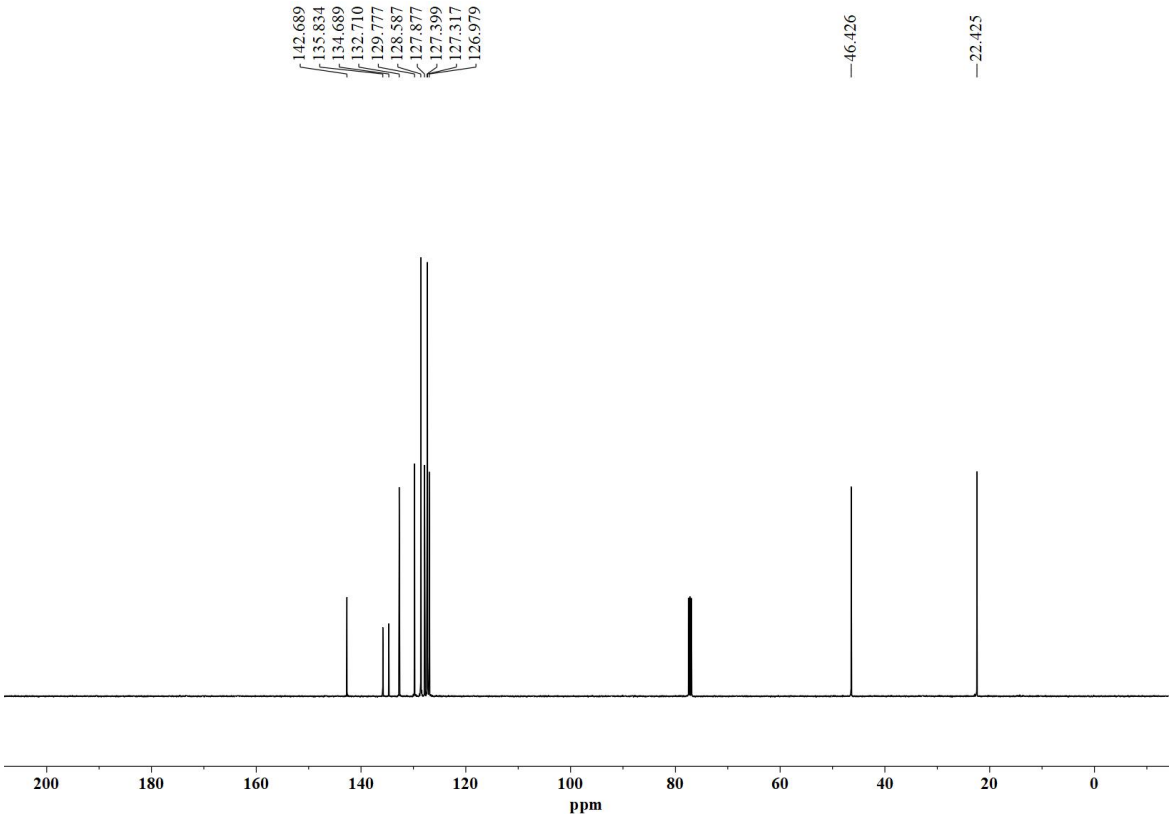

(b) ^{13}C NMR spectrum of (2-chlorophenyl)(1-phenylethyl)sulfane in $CDCl_3$.

Figure S28. NMR spectra of (1-phenylethyl)(p-tolyl)sulfane.

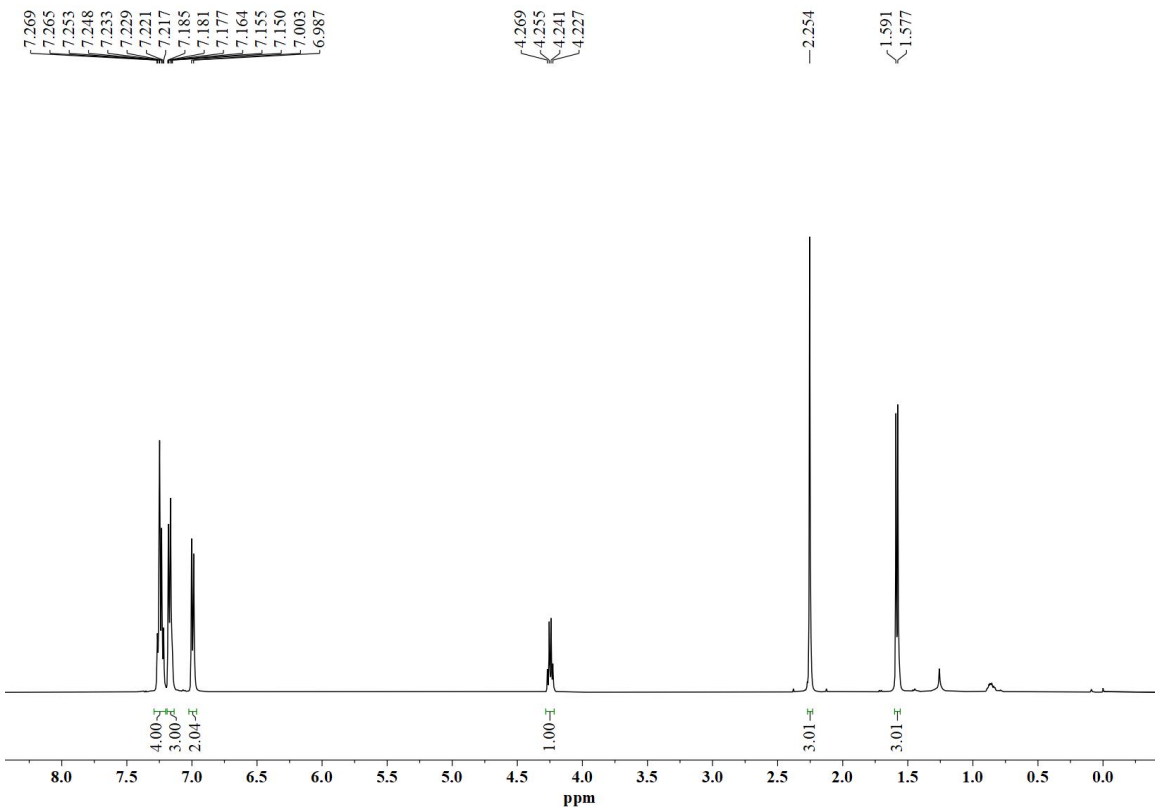

(a) ^{1}H NMR spectrum of (1-phenylethyl)(p-tolyl)sulfane in $CDCl_3$.

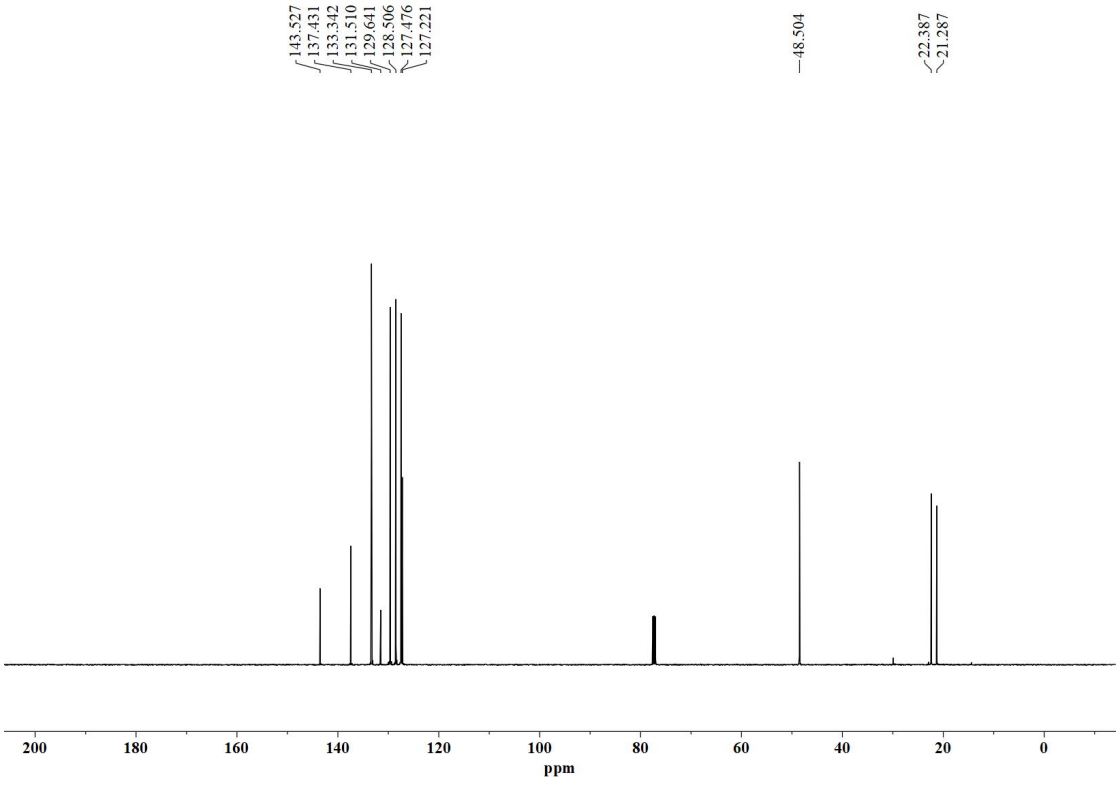

(b) ^{13}C NMR spectrum of (1-phenylethyl)(p-tolyl)sulfane in $CDCl_3$.

Figure S29. NMR spectra of (4-methoxyphenyl)(1-phenylethyl)sulfane.

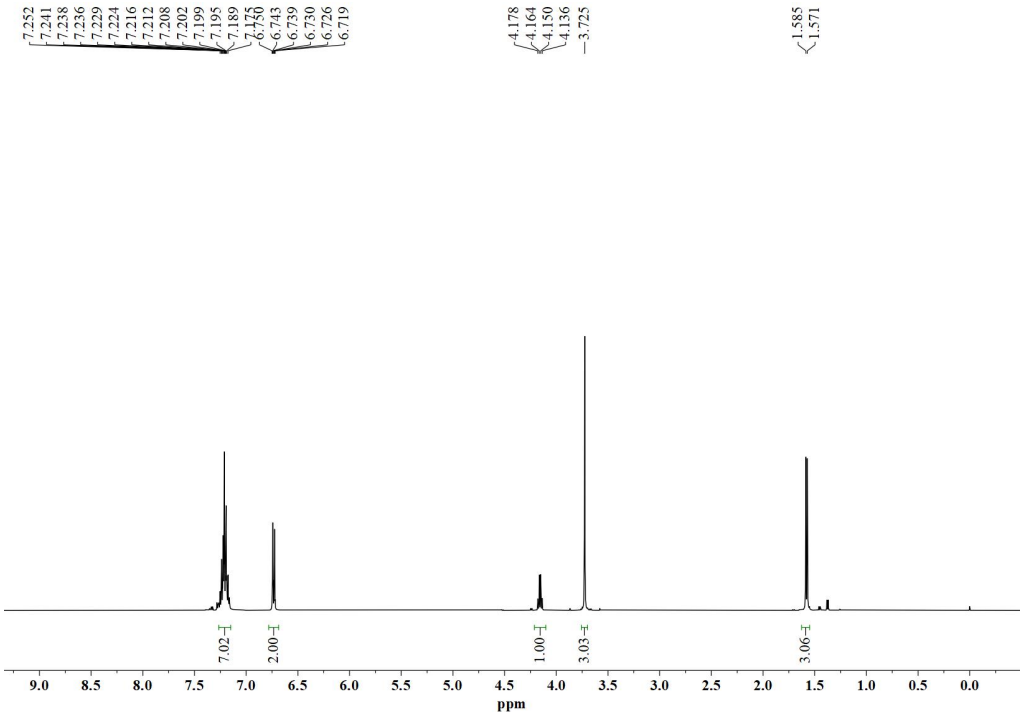

(a) ^{1}H NMR spectrum of (4-methoxyphenyl)(1-phenylethyl)sulfane in $CDCl_3$.

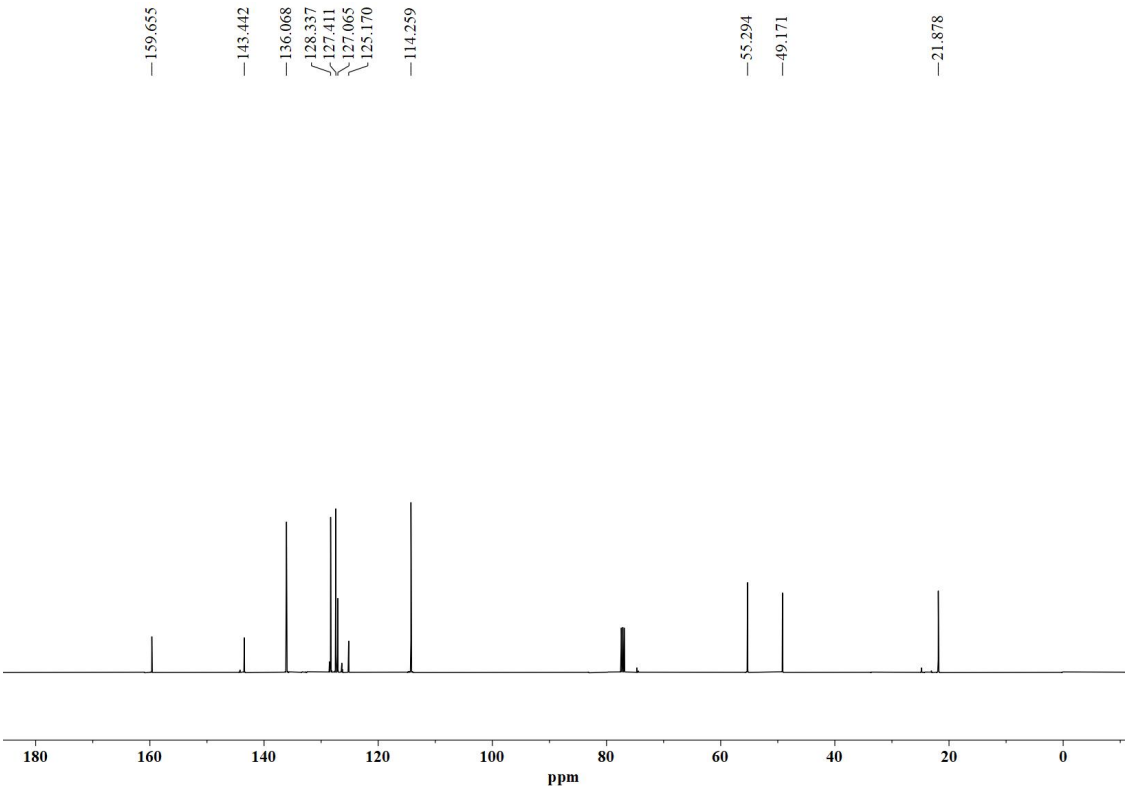

(b) ^{13}C NMR spectrum of (4-methoxyphenyl)(1-phenylethyl)sulfane in $CDCl_3$.

Figure S30. Spectroscopic data (HPLC trace).

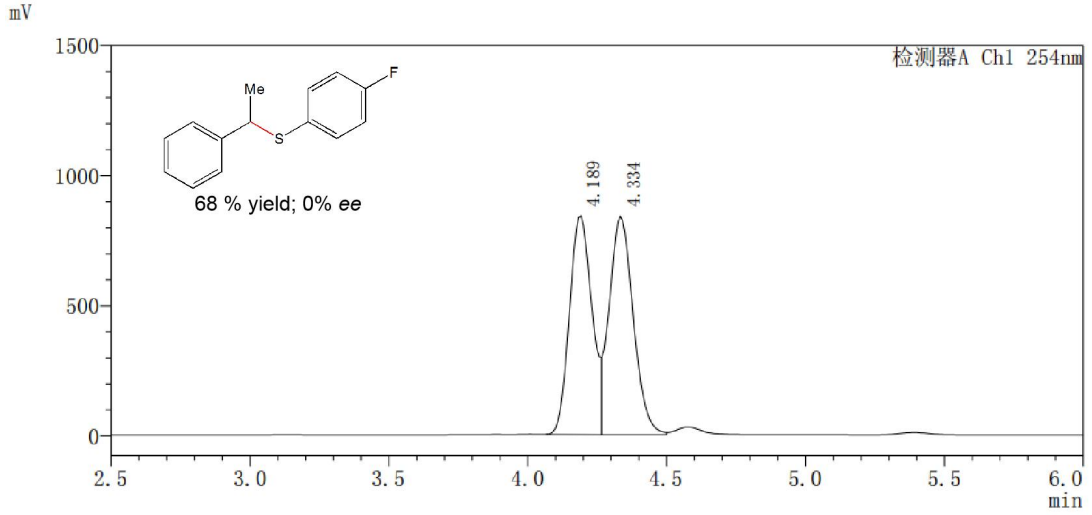

PDA Ch1 254 nm

Peak#	Resolution time	Area	Height	Concentration %
1	4.189	4831633	840985	49.155
2	4.334	4997653	839813	50.845
Total		9829286	1680797	100

Figure S31. NMR data and spectra of the isolated ether.

^{1}H NMR (500 MHz, Chloroform-*d*) δ 7.39-7.33 (m, 7H), 7.29-7.25 (m, 3H), 4.90 (q, *J* = 6.5 Hz, 2H), 1.50 (d, *J* = 6.5 Hz, 6H).^{13}C NMR (126 MHz, Chloroform-*d*) δ 145.82, 128.53, 127.51, 125.40, 70.45, 25.18.

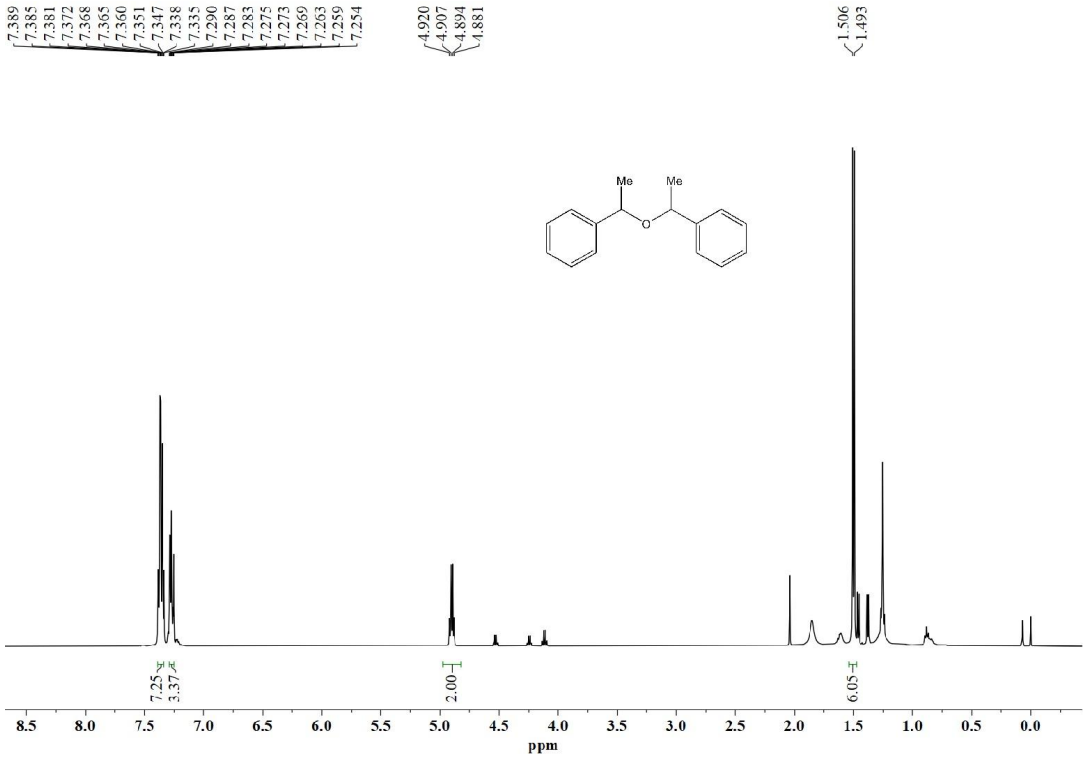

(a) ^{1}H NMR spectrum of the isolated ether in $CDCl_3$.

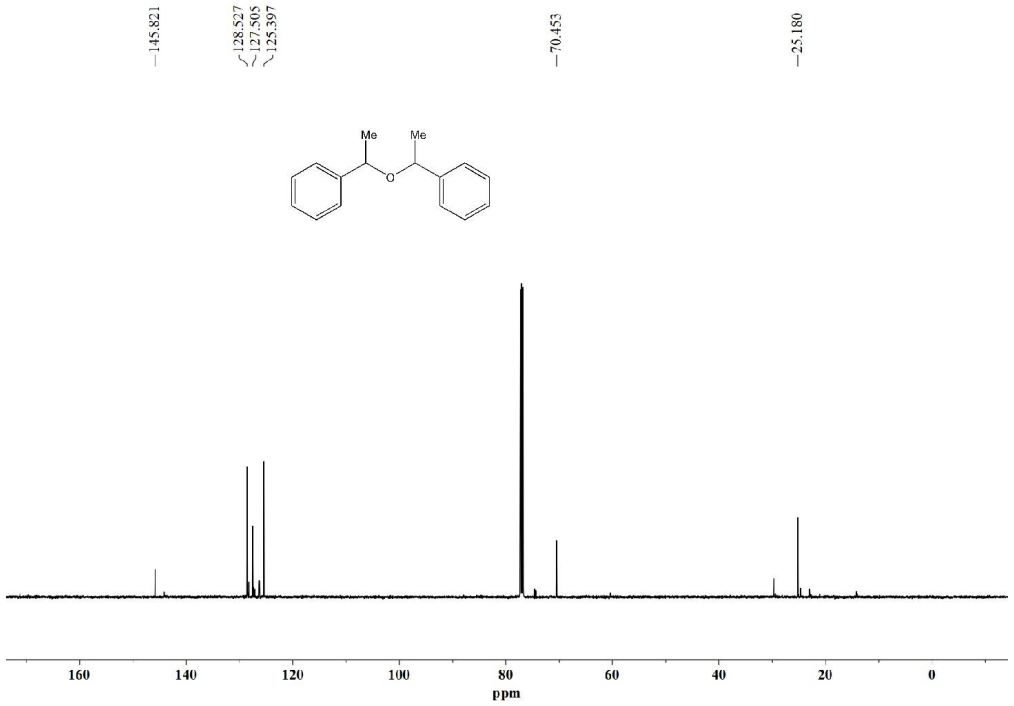

(b) ^{13}C NMR spectrum of the isolated ether in $CDCl_3$.

Reference:

[1] Y. Leng, J. Wang, D. R. Zhu, X. Q. Ren, H. Q. Ge and L. Shen, *Angew. Chem. Int. Ed.,* 2009, **48**, 168-171.